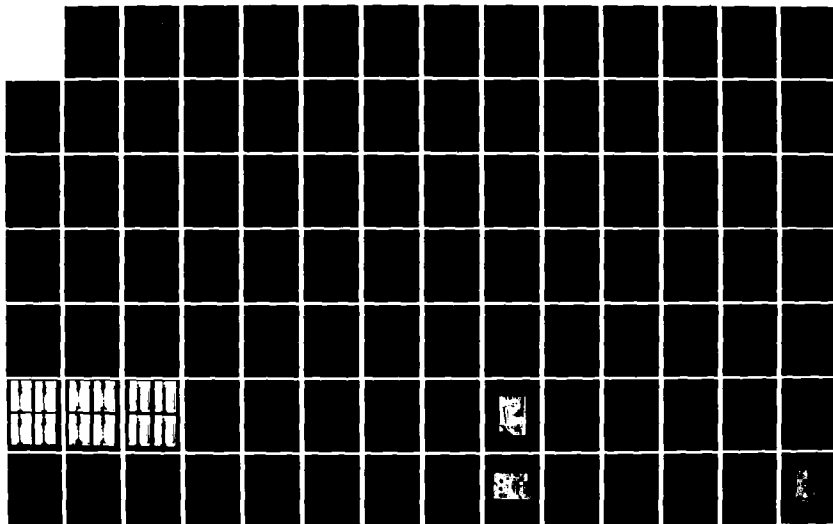


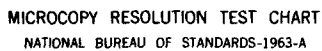
AD-A121 510

CROSS FLOW BOILING IN TUBE BUNDLES/ CARNegie ME
UNIV PITTSBURGH PA DEPT OF MECHANICAL ENGINEERING
S YAO OCT 82 N00014-79-C-0623

UNCLASSIFIED

F/G 20/13 NL





MICROCOPY RESOLUTION TEST CHART
NATIONAL BUREAU OF STANDARDS-1963-A

(12)

Cross Flowing Boiling in Tube Bundles

Annual Technical Report
October 1982

AD A121510

S.C. Yao
Associate Professor
Department of Mechanical Engineering
Carnegie-Mellon University
Pittsburgh, PA 15213

Prepared for
M.K. Ellingsworth, Program Monitor
The Office of Naval Research
Arlington, VA 22217

DTIC
SELECTED
NOV 17 1982
A

Under Contract No. N00014-79-C-0623, Work Unit 09-436
Approved for public release; distribution unlimited.
Reproduction in whole or in part is permitted for
any purpose of the United States Government.

DTIC FILE COPY

82 11 17 019

REPORT DOCUMENTATION PAGE		READ INSTRUCTIONS BEFORE COMPLETING FORM
1. REPORT NUMBER N00014-79-C-0623-1982A	2. GOVT ACCESSION NO. AD A121 570	3. RECIPIENT'S CATALOG NUMBER
4. TITLE (and Subtitle) CROSS FLOW BOILING IN TUBE BUNDLES		5. TYPE OF REPORT & PERIOD COVERED Annual Technical Report Aug. 1, 1981 to Aug. 1, 1982
		6. PERFORMING ORG. REPORT NUMBER
7. AUTHOR(s) Shi-Chune Yao		8. CONTRACT OR GRANT NUMBER(s) N00014-79-C-0623
9. PERFORMING ORGANIZATION NAME AND ADDRESS Dept. of Mechanical Engineering Carnegie-Mellon University Pittsburgh, PA 15213		10. PROGRAM ELEMENT, PROJECT, TASK AREA & WORK UNIT NUMBERS Program Element 6115-3N Project RR02403, Task Area RR0240302, Work Unit NR097-436
11. CONTROLLING OFFICE NAME AND ADDRESS Office of Naval Research 800 N. Quincy Street Arlington, VA 22217		12. REPORT DATE October 1982
14. MONITORING AGENCY NAME & ADDRESS (if different from Controlling Office)		13. NUMBER OF PAGES 60
		15. SECURITY CLASS. (of this report)
		15a. DECLASSIFICATION/DOWNGRADING SCHEDULE Unclassified
16. DISTRIBUTION STATEMENT (of this Report) Approved for public release; distribution unlimited.		
17. DISTRIBUTION STATEMENT (of the abstract entered in Block 20, if different from Report) Same as Block No. 16.		
18. SUPPLEMENTARY NOTES		
19. KEY WORDS (Continue on reverse side if necessary and identify by block number) Boiling Heat Transfer, Dryout, Corrosion, Tube Bundles		
20. ABSTRACT (Continue on reverse side if necessary and identify by block number) This report contains two main subjects. One is the newly started investigation of cross flow boiling in tube bundles. The heat transfer information at this condition is of significant importance to horizontal steam generator design. The other one is the continuation of the research on boiling heat transfer in confined spaces. The research on cross flow boiling in tube bundles has been started. The Freon loop has been modified for higher flow and higher two phase quality. The test		

DD FORM 1 JAN 73 1473

EDITION OF 1 NOV 63 IS OBSOLETE
S/N 0102-LF-014-6601

UNCLASSIFIED

SECURITY CLASSIFICATION OF THIS PAGE (When Data Entered)

UNCLASSIFIED

SECURITY CLASSIFICATION OF THIS PAGE (When Data Entered)

section design is finished and is under fabrication presently. The new instrumentation system is also established. The test matrix has been planned.

The research on boiling in confined spaces proceeds steadily. This problem is of great importance to the boiling induced corrosion in the steam generator crevices between the tube and the support plate. In the report of 1981, detailed results were presented for analysis of single phase flow, two phase flow, and dryout in crevices. Experimental results of boiling and dryout in crevices with closed bottom were also reported. In this report of 1982, the results of forced convective boiling heat transfer and critical heat flux in crevices are presented. The status of research on boiling in horizontal crevices is also described here.



A

UNCLASSIFIED

SECURITY CLASSIFICATION OF THIS PAGE (When Data Entered)

CROSS FLOW BOILING IN TUBE BUNDLES

Annual Technical Report

October 1982

S.C. Yao
Associate Professor
Department of Mechanical Engineering
Carnegie-Mellon University
Pittsburgh, PA 15213

Prepared for

M.K. Ellingsworth, Program Monitor
The Office of Naval Research
Arlington, VA 22217

Under Contract No. N00014-79-C-0623, Work Unit 097-436
Approved for public release; distribution unlimited.
Reproduction in whole or in part is permitted for
any purpose of the United States government.

TABLE OF CONTENTS

	<u>Page</u>
Summary	i
Conclusion	ii
Publications Resulted From the Present Research	iii
1. Critical Heat Flux of Forced Convective Boiling in Confined Spaces	1
2. Heat Transfer of Forced Convective Boiling in Confined Spaces	23
3. Pool Boiling in Horizontal Annular Crevices	44
4. Cross Flow Boiling in Tube Bundles	49
Distribution List	56

SUMMARY

→ This report contains two main subjects. One is the newly started investigation of cross flow boiling in tube bundles. The heat transfer information at this condition is of significant importance to horizontal steam generator design. The other one is the continuation of the research on boiling heat transfer in confined spaces.

The research on cross flow boiling in tube bundles has been started. The freon loop has been modified for higher flow and higher two phase quality. The test section design is finished and is under fabrication presently. The new instrumentation system is also established. The test matrix has been planned.

The research on boiling in confined spaces proceeds steadily. This problem is of great importance to the boiling induced corrosion in the steam generator crevices between the tube and the support plate. In the report of 1981, detailed results were presented for analysis of single phase flow, two phase flow, and dryout in crevices. Experimental results of boiling and dryout in crevices with closed bottom were also reported. In this report of 1982, the results of forced convective boiling heat transfer and critical heat flux in crevices are presented. The status of research on boiling in horizontal crevices is also described here. ←

CONCLUSION

The critical heat flux of forced convective boiling in confined space is generally lower than that of channels with conventional dimensions. For higher mass flux the CHF is higher. When the gap size decreases the CHF also decreases. The existing CHF correlations do not predict the data well. However, modification with the inclusion of the gap Bond number is able to fit the data. The Ahmad's correlation was modified for small gaps and for short channels. Our experimental data falls within $\pm 20\%$ of this modified correlation.

The heat transfer of forced convective boiling in confined space is generally higher than that of channels with conventional dimensions. When the wall superheat is low, the boiling curve shows higher heat flux at higher mass flux. However, at high wall superheat the boiling is fully developed. The effect of mass flux to boiling heat transfer becomes negligible. When the gap size decreases the heat transfer increases. Through visual observation, it is concluded that the increasing of heat transfer is due to the effective thin film evaporation beneath the squeezed (or called deformed) bubbles in the confined space. The boiling phenomena can be classified into three regimes: non-deformed bubbles, isolated deformed bubbles, and coalesced deformed bubbles. The boiling regimes can be identified in terms of Bond number and Boiling number of the system.

The present results will be useful for the design of the tube-to-baffle crevices in steam generators. The new correlations can be included into the computer program developed last year for more precise modeling of boiling in crevices.

The studies on boiling in horizontal crevices and on cross flow boiling in tube bundles proceed smoothly. The results will be available in the next year.

PUBLICATIONS RESULTED FROM THE PRESENT RESEARCH

1. S.C. Yao and Y. Hung, "Analysis of Fluid Flow and Heat Transfer in Heat Exchanger Tube-to-Baffle Clearances," ASME paper 81-WA/HT-10.
2. S.C. Yao and Y. Hung and J. Tang, "Analysis of Dryout in Steam Generator Crevices," ASME paper 81-WA/NE-2.
3. S.C. Yao and Y. Hung, "Heat Convection in Annular Type Crevices," Journal of Heat Transfer, Trans. ASME, Vol. 104, No.3, pp. 403-409, 1982.
4. S.C. Yao and Y. Chang, "A Scientific Movie - Visual Study of Boiling in Narrow Gaps with Closed Bottom," presented at 7th International Heat Transfer Conference, Munich, 1982.
5. Y. Chang and S.C. Yao, "Critical Heat Flux of Vertical Narrow Annuli with Closed Bottoms," accepted by Journal of Heat Transfer, Trans., ASME.
6. S.C. Yao and Y. Chang, "Pool Boiling Heat Transfer in Confined Space," accepted by Int. Journal of Heat Mass Transfer.

CHAPTER 1
CRITICAL HEAT TRANSFER
OF
FORCED CONVECTIVE BOILING IN CONFINED SPACES

NOMENCLATURE

Bo	Bond number for the gap, defined in equation (7)
CHF	Critical heat flux
D	Hydraulic equivalent diameter = $4 \times \text{flow area} / \text{wetted perimeter}$
D_{he}	Heated equivalent diameter = $4 \times \text{flow area} / \text{heated perimeter}$
E	Defined in equation (4)
G	Mass flux
g	Acceleration of gravity
H_{CHF}	Enthalpy of the fluid at critical heat flux
H_{in}	Enthalpy of liquid at inlet
H_l	Enthalpy of saturated liquid
ΔH_{in}	$H_l - H_{in}$
L	Heated length
P	Pressure
q_{CHF}	Critical heat flux
q_{Max}	Maximum critical heat flux = $GD_{he}(\lambda + \Delta H_{in})/4L$
W	Modified q_{CHF}/q_{Max} , defined in equation (8)
x_{CHF}	Quality of the fluid at critical heat flux

GREEK SYMBOLS

ρ_l	Density of liquid phase
ρ_g	Density of vapor phase
μ_l	Viscosity of liquid phase
μ_g	Viscosity of vapor phase
γ	Defined in equation (6)
λ	Latent heat of vaporization
Ψ_{CHF}	CHF modeling parameter, defined in equation (5)
δ	Gap thickness
σ	Surface tension of liquid phase

CRITICAL HEAT FLUX OF FORCED CONVECTIVE BOILING IN CONFINED SPACES

INTRODUCTION

In many heat exchange devices boiling occurs in confined spaces. For example, in steam generators, mechanical clearance is provided between the heating tube and the support-plate where the tube runs through. Flow is retarded in the narrow passage of the clearance. When the liquid is highly subcooled, single-phase forced convection will occur in the crevice as shown in Figure 1-a. When the liquid is slightly subcooled or saturated, boiling may occur in the crevice as shown in Figure 1-b. The boiling in the narrow passage may lead to permanent dryout and the accumulation of corrosive concentration at the dryout boundary. In order to prevent the dryout and the subsequent corrosion induced failure of the heating tube, an understanding of the fluid motion and heat transfer behavior in confined spaces will be of significant value to the design of the heat exchange devices.

Boiling in confined spaces may be viewed as a special case of the conventional boiling. The behavior of the CHF (Critical Heat Flux) in confined spaces can also be considered as an extension of the conventional CHF phenomena. Existing literature information on confined spaces boiling is scarce. Therefore, it is adequate to review the related conventional CHF behavior briefly.

A large number of experimental investigations on the CHF of forced

convective boiling in annuli have been performed and correlations for predicting the CHF have been proposed. Barnett [1] compiled 724 experimental data at the pressure of 6.9 MPa from 8 sources on the CHF of water in annuli where the inside rod is heated and the shroud tube is unheated. Latter Barnett [2] compiled additional 106 new data points from 3 other sources at the same pressure. Janssen et al. [3] conducted experiments of water at the pressure from 4.14 to 10.0 MPa, while the study of Litter [4] included experiments of water at the pressure from 5.17 to 6.9 MPa. Tolubinskiy et al. [5] presented an analysis of CHF data in annuli of 0.5 and 4 mm gaps with a forced flow of subcooled water. Some other studies have also been done on fluids different from water. Stevens et al. [6] reported experiments using Freon-12 at the pressure from 0.81 to 1.07 MPa. Ahmad et al. [7] presented 418 experimental data points for Freon-12 at pressure from 1.07 to 1.64 MPa.

A number of researchers have developed empirical correlations for CHF data. Barnett [1], Janssen et al. [3], Tong et al. [8], and Hewitt [9] have developed correlations for the CHF of water flowing in annuli with the inside tube heated. Some of the approaches were based upon mechanistic analyses of physical models, but the majority of the reported correlations were dimensional equations applying to specific fluid, most commonly water, in a limited range of conditions.

Few successful attempts have been made in developing correlations applicable to a wide range of conditions and to a variety of fluids. Bernath [10] and Gambill [11] developed correlations which apply only to the subcooled boiling CHF. Katto [12] used an analytical procedure he developed

for analyzing the CHF in round tubes [13], and obtained a graphical correlation for the CHF in annuli. Shah [14] compiled 39 data points and also presented a general correlation. His correlation had been developed in graphical form and is not simply translated into mathematical expressions. This correlation did not provide a satisfactory fit for gaps smaller than 0.5 mm. Using the uniqueness conditions of q_{CHF} , x_{CHF} , H_{CHF} and dimensional analysis, Ornatskiy et al. [15] developed a generalized correlation for water. Ahmad and Groeneveld [16] used Ahmad's compensated distortion model [17] to develop a CHF correlation for annular geometries that was independent of fluid type. This approach provides encouraging results and suggests a feasible means to predict the CHF with reasonable accuracy over the range of conditions presented in [16].

However, the range of data analyzed in reference [16] is not broad enough to consider the technique as having been verified for general applicability. Due to the complexity of the process, unavailability of detailed information on the mechanism of heat transfer, and differences in experimental techniques, none of the existing experimental studies and suggested techniques for correlating experimental data can be generally fit to the entire set of data for various annuli over a wide range parameters.

A number of experiments have been performed in pool boiling study. Katto and Yokoya et. al [18, 19] investigated confined space boiling of saturated water on a horizontal flat heated plate. A movable optical assembly was placed above the heated surface and had a small gap in between. They suggested that the dryout condition in confined space is a balance between the consumption of the liquid on the heated surface and the supplying of the

liquid between the intermittent jetting of vapor mass. Ishibashi and Nishkawa [20] conducted the boiling experiment for a vertical annulus with open ends. It was postulated that there are two distinct boiling regimes, each having different heat transfer characteristics. No quantitative information for dryout had been obtained. Jensen, Cooper and Bergles [21] performed experiments of boiling of an horizontal tube within constrain. The increase in the heat transfer was also explained by the thin film evaporation. The CHF was found to be directly proportional to the gap size and inversely proportional to the length of annulus. Yao and Chang [22] presented a series of systematic investigations of pool boiling heat transfer in vertical narrow annuli with closed bottoms. They found that the Bond number is important in characterizing the boiling behavior into three different boiling regimes.

Building on the experimental results and conclusions of pool boiling in confined spaces by the above researchers, the objectives of the present research are to understand the governing mechanisms of forced boiling in confined spaces; to study the effects of the space confinement and the mass flux on the CHF; and to develop a generalized correlation for uniformly heated cylindrical annuli under uniform heat flux with narrow gaps over wide ranges of parameters.

EXPERIMENTAL APPARATUS AND PROCEDURE

The experimental set-up consists of a narrow annular test section placed in a closed loop of Freon-113 at slightly pressurized conditions.

Test Loop

As shown in Figure 2, Freon-113 is circulated by a centrifugal pump through the control valves, the turbine flow meter, the preheaters, the annular test section, the condenser, and then back to the suction side of the pump. The flow rate in the annular test section is regulated by adjusting the bypass control valves, and the desired system pressure is maintained through Nitrogen gas in the glass container. Almost all of the loop is constructed of 304 stainless steel piping.

The bulk fluid temperature at the inlet of the test section and at six other locations in the loop are measured with calibrated J-type thermocouples. These thermocouples are read from a digital temperature reader(Omega Model 403A-C) through a selecting switch.

The inlet conditions to the test section are adjusted by the power input to the preheaters and the throttling of the flow at the regulating valve. Both preheaters are of Chromalox immersion type Model ARMTO-3605T2. Each preheater has a rated output of 6 KW. The power to the heaters is regulated through a variable transformer which can be adjusted finely.

Test Section

The schematic of the test section is shown in Figure 3. The heated section is made of 304 stainless steel seamless tubing with 0.71 mm wall

thickness, 25.4 mm O.D., and the heated length is 76.2 mm. The top of the heated tube is thermally shrink-fitted to a copper tube which has the same O.D. as the heated section but with 1.42 mm wall thickness. The bottom of the heated tube is shrink-fitted to a copper rod. The D.C. current is measured from the voltage drop through a shunter.

The hollow quartz cylinders are milled to an outside diameter of 63.5 mm with the inside diameters 26.04, 27.00, and 30.56 mm respectively to form different gap sizes with respect to the heating tube. Both the inside and the outside surfaces of the quartz are polished to a 50-80 finish to permit visual observation of the annulus. Three of the annuli tested are 76.2 mm long with the gap sizes of 0.32, 0.80, 2.58 mm, respectively. The concentric annulus between the heating tube and the quartz-cylinder is maintained by two spacers located at the top and the bottom of the quartz.

The pressure at the inlet of the test section is measured at the lower plenum and is indicated on a pressure gauge ranging from 0.1 to 0.3 MPa. The pressure drop through the annulus is measured using a calibrated pressure transducer (Model PB415D-13) which is connected to a strip chart recorder (Sanborn Model 321).

A pair of traversable thermocouples as shown in Figure 4 are used to measure the inside wall temperature of the heating tube. Two J-type, stainless steel sheathed, ungrounded thermocouples of 0.81mm diameter are pressed against the inner-wall by plate-springs with a force of 5.87 Newtons. The thermocouples are calibrated but the temperature measurement accuracy is limited by the digital temperature display to $\pm 0.28^{\circ} \text{C}$. The outside surface temperature is calculated from one-dimensional steady state heat conduction

equation [23, 24] over the tube wall. The same heating tube is used for all the tests. The heated surface is polished before each test with a # 320 sandpaper. The thermocouples are located 6.35 mm below the top opening of the narrow annulus to detect the early critical heat flux.

Prior to the collection of data, the loop was filled and degassed. Then, the inner tube is gradually heated by the D.C. power. The steady states were achieved within 3 minutes after any change of heat flux. Data were taken then. During the test run of varying heat flux, the mass flow rate, the inlet conditions and the system pressure are held constantly.

RESULTS AND DISCUSSION

Boiling crisis is a sudden drop of heat transfer coefficient occurring after a very high heat flux in nucleate boiling has been reached. This sudden drop of heat transfer coefficient will cause a surface temperature surge, if the heat flux to the heated surface is maintained constant. Therefore, the observation and the data taken for CHF here is the heat flux at which a sharp rise in surface temperature takes place.

The experiments are performed at steady states. The range of the test conditions are listed in Table 1. In order to get reliable information every data is repeated in three different tests at the same conditions. The maximum deviation of the CHF data for a same condition is found to be 3.02%. The maximum rate of heat loss at the inside of the tube by natural convection is estimated using the references [24,25] to be within 1.6 % of the total power.

Effect of Mass Flux

The data of CHF are presented in Figure 5 for various mass fluxes with the gap size as the parameter. With all other conditions fixed, the CHF is found to increase with the increasing of mass flux. This is apparently due to the increase of the flow turbulence and transverse fluid flow fluctuations at higher flow rates. Tolubinskiy et al. [26] pointed out that the CHF at conventional size flow channels is proportional to the velocity gradient near the wall layer. Therefore, the increase of the mass flux will increase the CHF. In the present investigation, although the gap is very small the wall velocity gradient seems also playing an apparent role in the CHF values.

The limiting situation of the CHF will correspond to the condition that the exit quality is at 1.0 that the gap flow occurs at the exit point. Developed from the energy balance, these conditions are shown on the Figure 5 as straight lines. They can be considered as the limits of the present data trend at low mass flux.

Effect of Gap Size

As shown in Figure 5, the CHF decreases with the reduction of gap size. In narrow annuli, the geometry constraint affects the value of CHF. Closeness of the annuli walls interferes with disengagement of vapor from the heated surfaces. At higher heat flux levels, longer residence time of the vapor mass in a small gap allows thin film evaporation to occur, this thin film evaporation causes dryout to occur at lower CHF levels than conventional large gap cases.

Gambill [11] observed that his correlation grossly over-predicted the CHF when the gap was reduced below 2 mm. Tolubinskiy et al. [27] concluded that the CHF was independent of gap width provided it was greater than 1 mm but the CHF decreased sharply when the gap became less than 1 mm. Shah [14] presented his correlation and compared to the data for gap sizes ranging from 0.5 to 11.1 mm. No maxima was found at 4mm as had been noted by Moeck et al. [28]. The correlation of Shah [14] was in agreement with the experimental data at gap sizes of 1.5 mm and larger. The deviation between the experimental data and his prediction increased sharply when the gap was reduced below 1.5 mm, especially for the gap sizes below 0.5 mm. Considering the general inconsistency between the reported experimental data of narrow gaps and the predictions suggested by many researchers, the author intended to improve the CHF correlations at the condition of narrow gap sizes.

CHF Correlation

A rather generalized CHF correlation for annular geometries which is valid for various kinds of fluids has been developed by Ahmad [16], the correlation can be expressed as

$$q_{CHF}/q_{Max} = 1 - \exp[-0.025(\rho_l/\rho_g - 1)^{0.266} E(1 + \Delta H_{in}/\lambda)^{3.9/E^{1/2}}] \quad (1)$$

(for the range of gap sizes in between of 3.2 and 6.4 mm,
and the L/D ratio in between of 140 and 222.)

Where

$$q_{Max} = \text{Maximum critical heat flux} = GD_{he}(\lambda + \Delta H_{in})/4L \quad (2)$$

$$\Delta H_{in} = H_l - H_{in} \quad (3)$$

$$E = (L/D)^{0.715} \Psi_{CHF}^{0.866} \quad (4)$$

Ψ_{CHF} is a critical heat flux modeling parameter defined as

$$\Psi_{CHF} = [(GD/\mu_l)(\gamma^{1/2} \mu_l/\rho_l^{1/2} D)^{2/3} (\mu_l/\mu_g)^{1/8}] \quad (5)$$

$$\gamma = \left| \frac{\partial(\rho_l/\rho_g)}{\partial P} \right| \quad (6)$$

The present investigation involves data of 17 Freon-113 critical heat fluxes for 76.2 mm long annuli (inside diameter 25.4 mm, gap thickness 0.32, 0.80, and 2.58 mm) at 0.132 MPa, and mass fluxes from 124.0 to 1144.9 Kg/sec-m². These experimental data have been compared with the correlation of Ahmad [16] as shown in Figure 6. The comparison is also listed in Table 2. The mean deviation for the worst case of 0.32 mm gap size is 120 %. Moreover, for the case of 2.58 mm gap size the mean deviation is still very large (114 %). This is possibly because the L/D ratio in the large gap case is 15 which is much less than the minimum L/D ratio (140) in Ahmad's correlation.

The effect of the gap size is likely to be significant when it is smaller than, say, 1.5 mm. A natural explanation is that the bubbles experience severe geometric constrain at this condition. As observed from the photographs of the boiling at the condition of narrow gaps, the bubbles have been severely squeezed as the shape of pancakes between the walls. A non-dimensional parameter called Bond number can be used to relate the gap size δ and the capillary constant as

$$Bo = \delta / [\sigma / g(\rho_l - \rho_g)]^{1/2} \quad (7)$$

In some sense, the Bond number can also be related as the ratio of the gap size δ and the bubble departure diameter in the conventional pool boiling. Furthermore, the previous study of Yao and Chang [22] on the pool boiling in

narrow crevices indicated that the boiling regimes can be related with the Bond number of the system at low heat flux. Therefore, the Bond number will be used to correlate the data for the effect of the gap size.

Since the correlation of Ahmad is generally valid in wide ranges of conditions, the effects of the gap size and the heated length to hydraulic diameter ratio will be correlated as an extra correlation term multiplying on the Ahmad's correlation [16]. That is

$$W = f(Bo, L/D) * (q_{CHF}/q_{Max}) \quad (8)$$

Where

$$f(Bo, L/D) = [1 - 0.7 \exp(-Bo)] [1 - 0.8 \exp(-0.035 L/D)] \quad (9)$$

The details of the modification function is shown in Figure 7 with the conditions of the present experiments indicated as points in the same figure. When the gap and the ratio of the heated length to hydraulic diameter are large enough, i.e. $Bo \gg 1$ and $L/D \gg 1$, Equation (8) is identical with the original correlation proposed by Ahmad [16].

The present data and the data of Barnett reported in [16] are listed in Table 2, the modified correlation (8) substantially improves the original correlation of (1). The comparisons of predicted and experimental results are shown in Figure 8. The mean deviation of the predicted CHF with respect to the experimental data is 6.86 %, 11.38 %, and 11.33 % for the gap sizes 0.32, 0.80, and 2.58 mm respectively. The averaged deviation between all the experimental data (44 points) and the predictions of (8) is 9.4 % with the maximum deviation within 20 %. The ratios of the CHF data to the predicted CHF using the modified correlation (8) are also shown in Figure 9. Great improvement as compared with Figure 6 is observed.

CONCLUSIONS

The forced convective critical heat flux in confined spaces has been studied for various gap sizes and mass fluxes. The CHF increases as the mass flux is increased. The CHF decreases as the gap size is decreased. The mechanism of dryout in a very narrow gap is dominated by thin film evaporation. At higher heat flux levels, longer residence time of the vapor mass in the very narrow gap allows thin film evaporation to occur. Therefore, this thin film evaporation causes dryout to occur at lower CHF levels than conventional large gap cases.

The Ahmad's correlation may be modified for the conditions of small gaps and low heated length to hydraulic diameter ratio. The modification is described as a correlation function which is based upon the Bond number of the gap size and the L/D ratio. The modified correlation presented in the present report has been compared to Barnett's data and the present experimental data with fairly good results. More data analysis for very thin annular gaps is needed to confirm the applicability of this modified correlation, and to establish a generalized correlation which can apply to a wide variety of fluids and a wide range of parameters.

REFERENCES

1. Barnett, P. G., "A Correlation of Burnout Data for Uniformly Heated Annuli and Its Use for Predicting Burnout in Uniformly Heated Rod Bundles," AEEW-R463, 1966.
2. Barnett, P. G., "A Comparison of The Accuracy of Some Correlations for Annuli and Rod Bundles," AEEW-R558, 1968.
3. Janssen, E., and Kervinen, J. A., "Burnout Conditions for Single Rod in Annular Geometry," GEAP-3899, 1963.
4. Little, R. B., "Dryout Tests on An Internally Heated Annulus with Variation of Axial Heat Flux Distribution," AEEW-R578, 1970.
5. Tolubinskiy, V. I., Litoshenko, A. K., and Shevtsov, V. L., "Critical Heat Flux Densities in Internally-Heated Annuli," Heat Transfer-Soviet Research, Vol.2, NO.6, 1970.
6. Stevens, G. F., Wood, R. W., and Pryzbyski, J., "An Investigation into The Effect of A Cosine Axial Heat Flux Distribution on Burnout in a 12 ft Long Annulus Using Freon-12," AEEW-R609, 1968.
7. Ahmad, S. Y., and Groeneveld, D. C., "Fluid Modeling of Critical Heat Flux in Uniformly Heated Annuli," International Symposium on Two-Phase Systems, Haifa, 1971, Paper 1-8, or AECL-4070, 1972.

8. Tong, L. S., Currin, H. B., and Engel, F. C., "DNB (Burnout) Studies in An Open Lattice Core," WCAP-3736, 1964.
9. Hewitt, G. F., Kearsy, H. A., and Collier, J. G., "Correlation of Critical Heat Flux for The Vertical Flow of Water in Uniformly Heated Channels," AERE-5590, 1970.
10. Barnett, P. G., "A Theory of Local-Boiling Burnout and Its Application to Existing Data," *Chem. Eng. Prog. Symp.*, Ser.30, 56, pp.95, 1960.
11. Gambill, W. R., "Generalized Prediction of Burnout Heat Flux for Flowing Subcooled Wetting Liquids," *Chem. Eng. Prog. Symp.*, Ser.59, 41, pp.71, 1963.
12. Katto, Y., "Generalized Correlations of Critical Heat Flux for The Forced Convection Boiling in Vertical Uniformly Heated Annuli," *Int. J. Heat Mass Transfer*, Vol.22, pp.575, 1979.
13. Katto, Y., "A Generalized Correlation of Critical Heat Flux for The Forced Convection Boiling in Vertical Uniformly Heated Round Tubes," *Int. J. Heat Mass Transfer*, 21, pp.1527, 1978.
14. Shah, M. M., "A General Correlation for Critical Heat Flux in Annuli," *Int. J. Heat Mass Transfer*, Vol.23, pp.225, 1980.
15. Ornatskiy, A. P., Chernobay, V. A., Perkov, S. V., and Vasil'yev, A. F., "Correlations of Data on Heat Transfer Crisis in Annuli on The

Basis of Flow Parameters at The Inlet," *Heat Transfer-Soviet Research*, Vol.8, No.3, 1976.

16. Ahmad, S. Y., and Groeneveld, D. C., "Fluid Modeling of Critical Heat Flux in Uniformly Heated Annuli," *Progress in Heat and Mass Transfer*, pp.45, 1972.
17. Ahmad, S. Y., "Fluid to Fluid Modeling of Critical Heat Flux : A Compensated Distortion Model," *Int. J. Heat Mass Transfer*, Vol. 16, pp.641, 1973.
18. Katto, Y., and Yokoya, S., "Experimental Study of Nucleate Pool Boiling in Case of Making Interference-Plate Approach to the Heating Surface," Third International Heat Transfer Conference, pp.219, 1966.
19. Katto, Y., Yokoya, S., and Teroka, K., "Nucleate and Transition Boiling in a Narrow Space Between Two Horizontal, Parallel Disk Surfaces," *Bulletin of JSME* 20 (143), 1977.
20. Ishibashi, E., and Nishikawa, K., "Saturated Boiling Heat Transfer in Narrow Space," *Int. J. Heat Mass Transfer*, Vol.12, pp. 863, 1969.
21. Jensen, M. K., Cooper, P. E., and Bergles, A. E., "Boiling Heat Transfer and Dryout in Restricted Annular Geometries," 16th National Heat Transfer Conference, *AIChE*, Paper No. AIChE-14, pp.205, 1976.

22. Yao, S. C., and Chang, Y., "Pool Boiling Heat Transfer in Confined Spaces," 7th International Heat Transfer Conference, 1982.
23. Lung, H., Latsch, K., and Rampf, H., "Boiling Heat Transfer to Subcooled Water in Turbulent Annular Flow," *Heat Transfer in Boiling*, Hemisphere Publishing Corporation, Washington, pp. 225, 1977.
24. Hennecke, D. K., and Sparrow, E. M., "Local Heat Sink on A Convectively Cooled Surface-Application to Temperature Measurement Error," *Int. J. Heat Mass Transfer*, Vol.13, pp.287, 1970.
25. Robert P. Benedict, "Graphical Heat-Transfer Estimation," *Electro-Technology*, pp.93, March 1964.
26. Tolubinskiy, V. I., Litoshenko, A. K., and Shevtsov, V. L., "Effect of Curvature on The Critical Heat Flux Density in Forced-Convection Flow," *Heat Transfer-Soviet Research*, Vol.5, No.1, 1973.
27. Tolubinskiy, V. I., Litoshenko, A. K., and Shevtsov, V. L., "Correlation of Experimental Data on Critical Heat Fluxes in Annular Channels," *Heat Transfer-Soviet Research*, Vol.1, No.1, pp.80, 1969.
28. Moeck, E. O., Matzner, B., Casterline, G. E., and Yuill, G. K., "Critical Heat Flux in Internally Heated Annuli of Large Diameter Cooled by Boiling Water at 1000 psia," Proceedings of the Third International Heat Transfer Conference, Vol.3, ASME, New York, pp.86, 1966.

Table 1. Range of Parameters for Operating Conditions

Working Fluid	Freon - 113
Geometry	Vertical upflow in concentric annuli with internal heating
System Pressure	0.132 MPa
Saturation Temp.	55.6° C
Material of heated tube	304 stainless steel seamless tube
O. D. of heated tube	25.4 mm
T/S Length	76.2 mm
Inlet Subcooling	1.21×10^4 J/kg
Variable Parameters :	
Gap Size	0.32 - 2.58 mm
Mass Flux	124.0 - 1144.9 kg/m ² sec

Table 2. Comparison between Ahmad's Correlation [16] and Eqn.(8)

(I)*. Working Fluid : Water ; System Pressure : 6.9 MPa

Heated Length : 1828.8 mm ; Gap Size : 5.7 mm

Mass Flux (kg/m ² sec)	Inlet Subcooling (10 ⁴ J/kg)	Measured CHF (KW/m ²)	% Error in Predicting CHF	
			Ahmad's correlation	EQN(8)
676.8	21.59	1642.44	-13.4	- 8.5
678.2	0.46	1254.69	-11.7	- 6.6
683.6	40.85	2008.13	-16.7	-12.0
697.2	8.82	1481.67	- 7.5	- 2.7
698.6	21.59	1639.29	-15.0	-10.1
709.4	26.46	1778.00	-13.4	- 8.6
710.8	0.93	1264.14	-13.2	- 8.0
717.6	34.12	2027.05	- 9.5	- 4.9
719.0	15.55	1547.87	-13.9	- 8.9
724.4	8.36	1434.38	-11.7	- 6.7
1077.8	16.71	2058.57	0.0	4.4
1098.1	26.23	2276.09	4.7	- 0.2
1109.0	10.21	1932.47	2.8	7.3
1346.8	18.11	2386.43	5.1	9.3
1368.6	27.16	2730.05	3.8	8.0
1387.6	11.84	2263.48	8.9	13.1
2007.4	3.25	2263.48	14.8	18.9
2010.1	17.41	2802.56	9.1	13.2
2011.4	27.62	3187.16	3.9	8.1
2015.5	10.45	2562.97	12.9	17.0
2023.7	29.71	3310.11	3.9	8.0
2029.1	9.05	2496.77	12.9	17.0
2623.0	26.23	3354.24	1.6	5.9
2678.7	16.94	3029.53	8.8	13.0
3287.6	13.23	2969.64	8.7	12.9
3317.5	3.95	2430.56	10.8	14.5
3370.5	27.85	3596.98	4.5	0.0

(II)**. Working Fluid : Freon-113 ; System Pressure : 0.132 MPa

Heated Length : 76.2 mm ; Inlet Subcooling: 1.21×10^4 J/kg

Gap Size (mm)	Mass Flux (kg/m ² sec)	Measured CHF (KW/m ²)	% Error in Predicting CHF	
			Ahmad's Correlation	EQN(8)
0.32	145.1	33.10	-139.0	-13.6
0.32	216.0	48.10	-112.3	- 0.9
0.32	381.6	63.83	-115.6	- 2.5
0.32	636.0	83.19	-105.5	- 2.3
0.32	890.4	88.09	-119.9	- 4.5
0.32	1144.9	92.03	-129.6	- 9.1
0.80	124.0	84.60	- 39.6	20.5
0.80	216.0	101.20	- 48.1	15.7
0.80	381.6	119.20	- 54.5	12.1
0.80	636.0	122.30	- 77.9	- 1.3
0.80	890.4	129.10	- 87.3	- 6.6
0.80	1144.9	132.80	- 97.0	-12.1
2.58	216.0	116.00	- 80.6	11.0
2.58	381.6	128.50	- 95.0	3.9
2.58	636.0	138.50	-114.0	- 5.5
2.58	890.4	141.00	-136.5	-16.6
2.58	1144.9	150.80	-142.7	-19.7

* (I). Barnett's data [2]

** (II).Present Experimental data

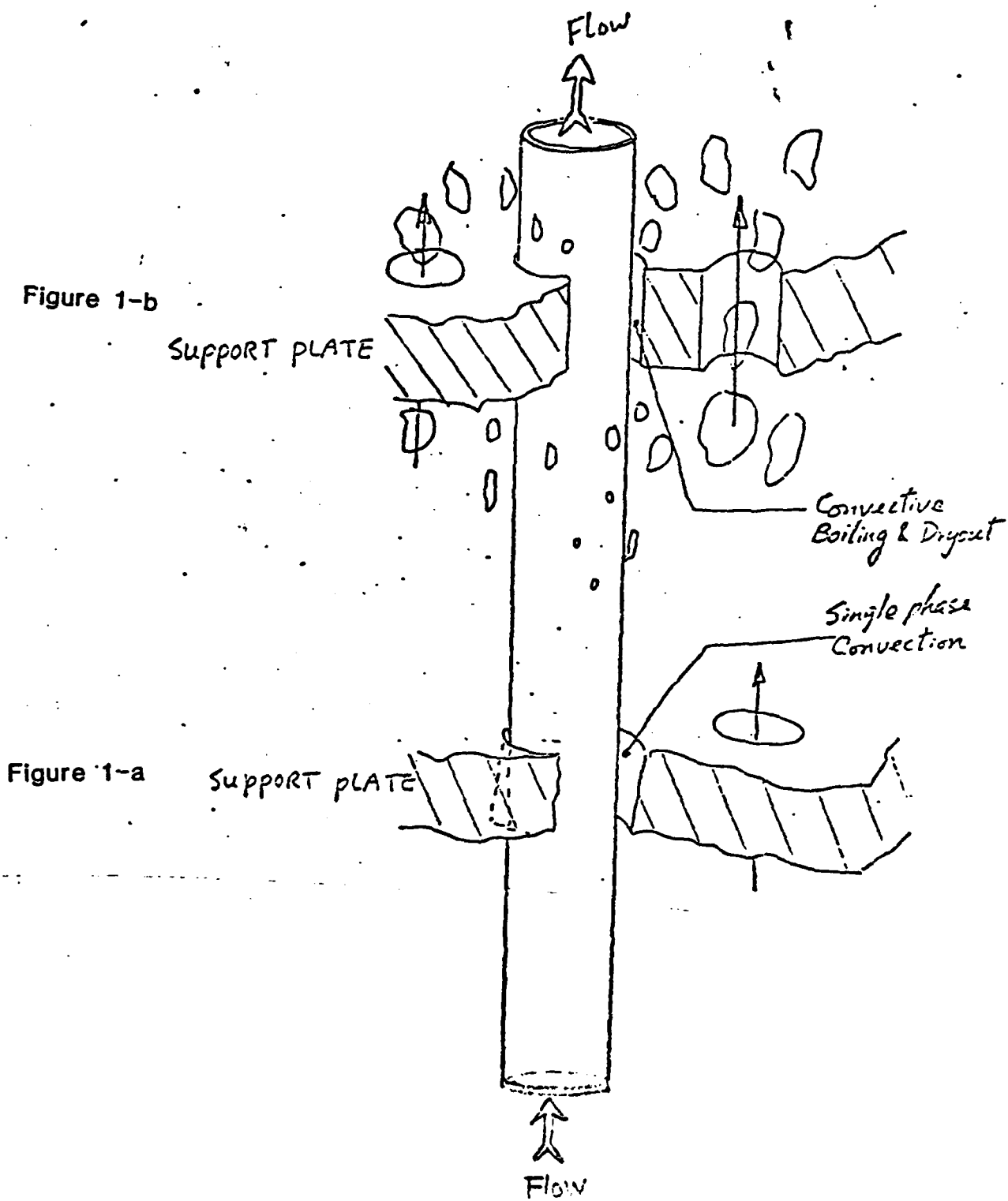


Figure. 1

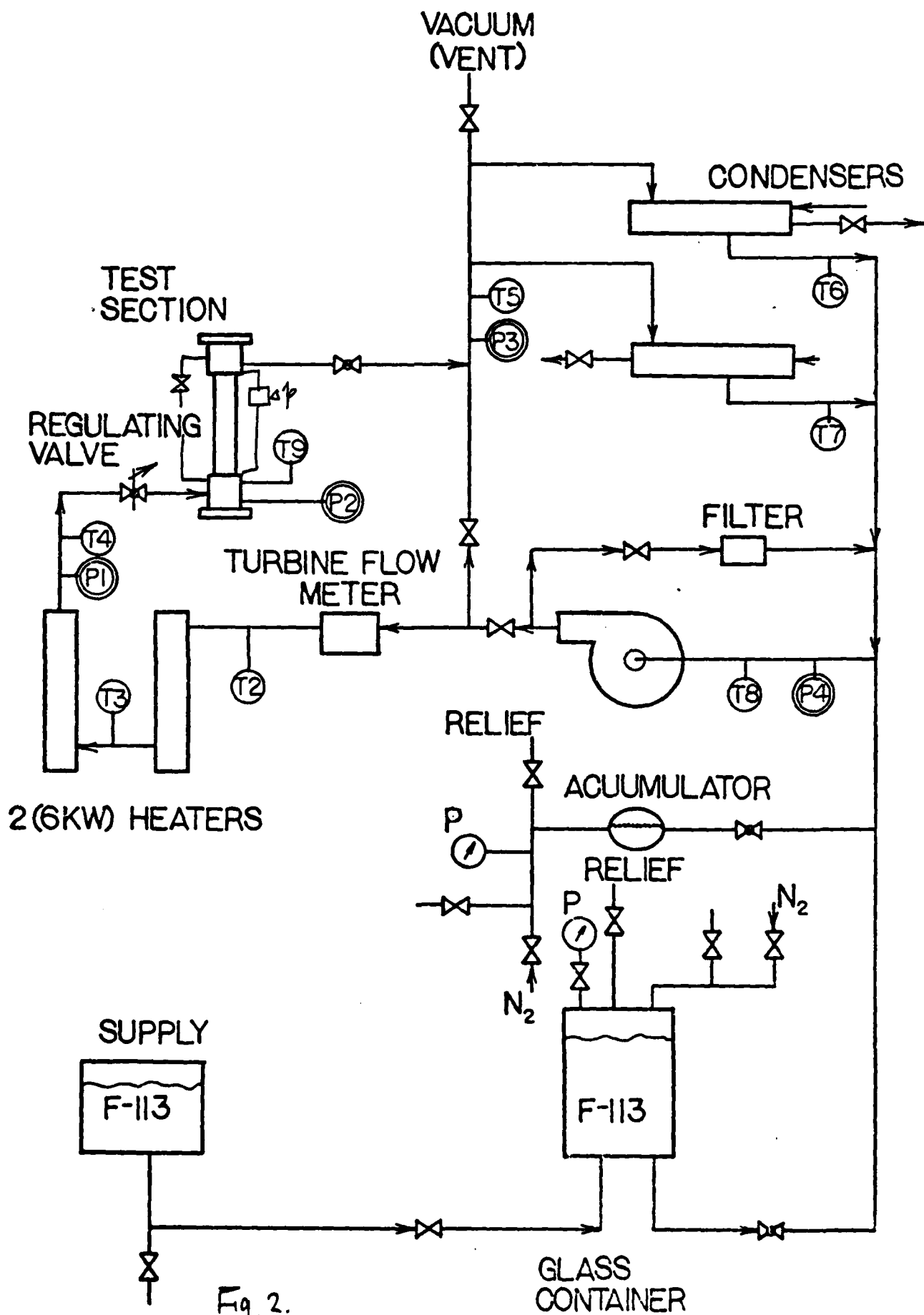


Fig. 2.

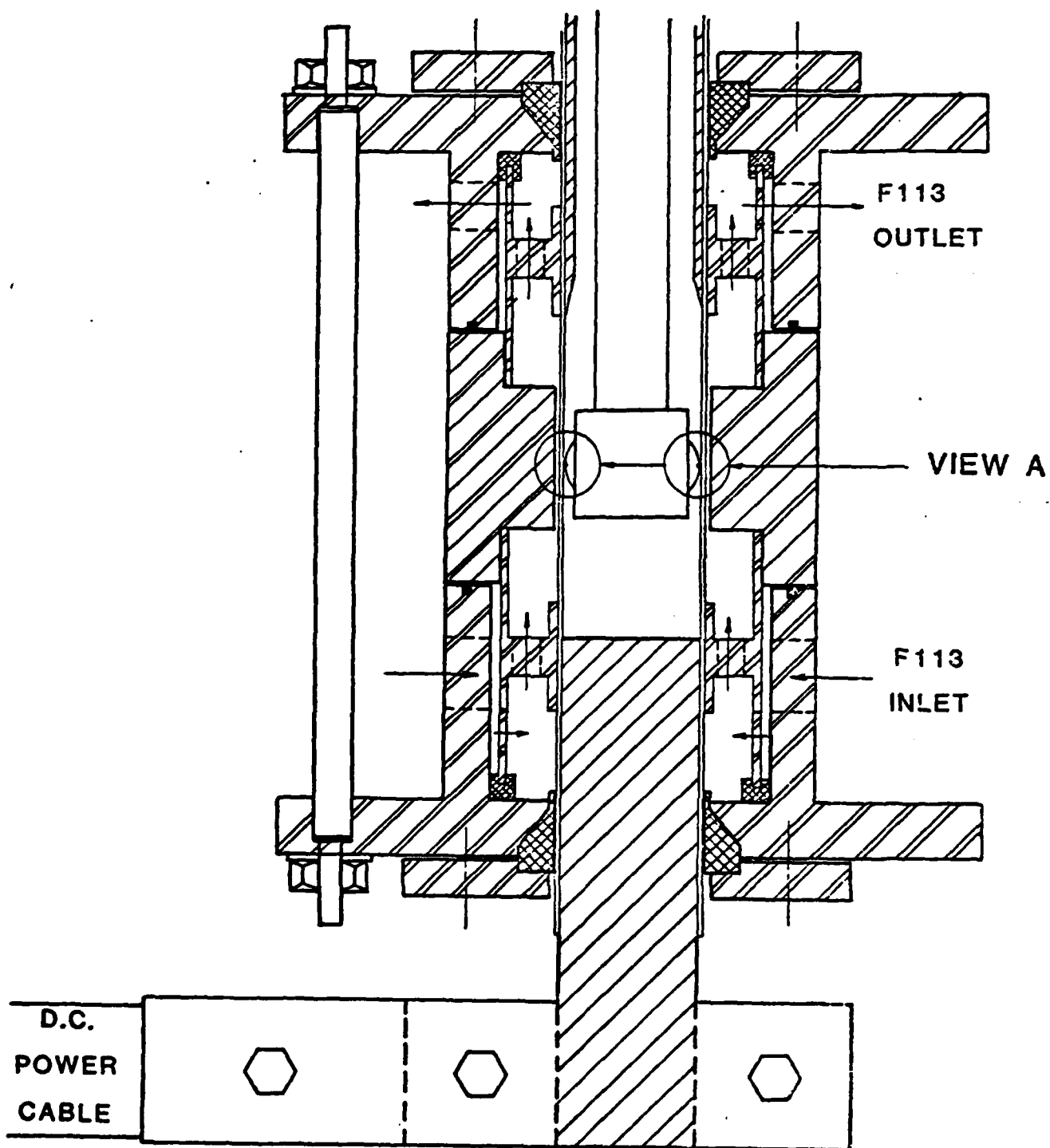


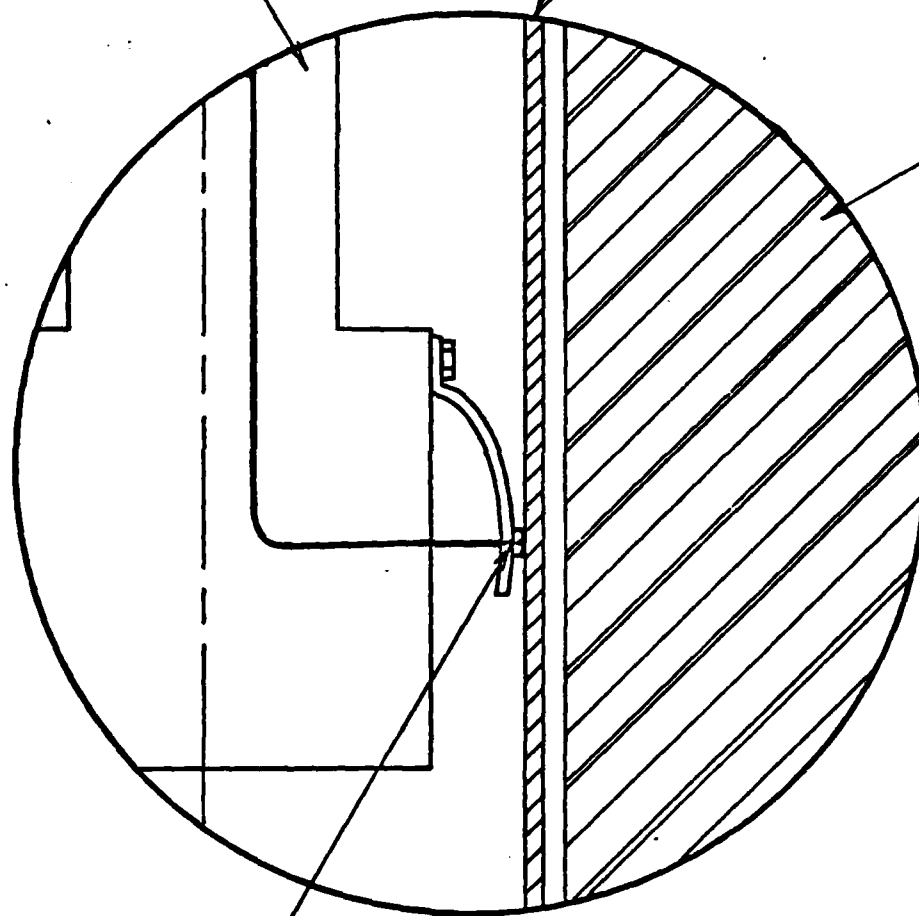
Fig 3.

Movable sensor
and rod

Heated stainless steel tube

Quartz

Thermocouple

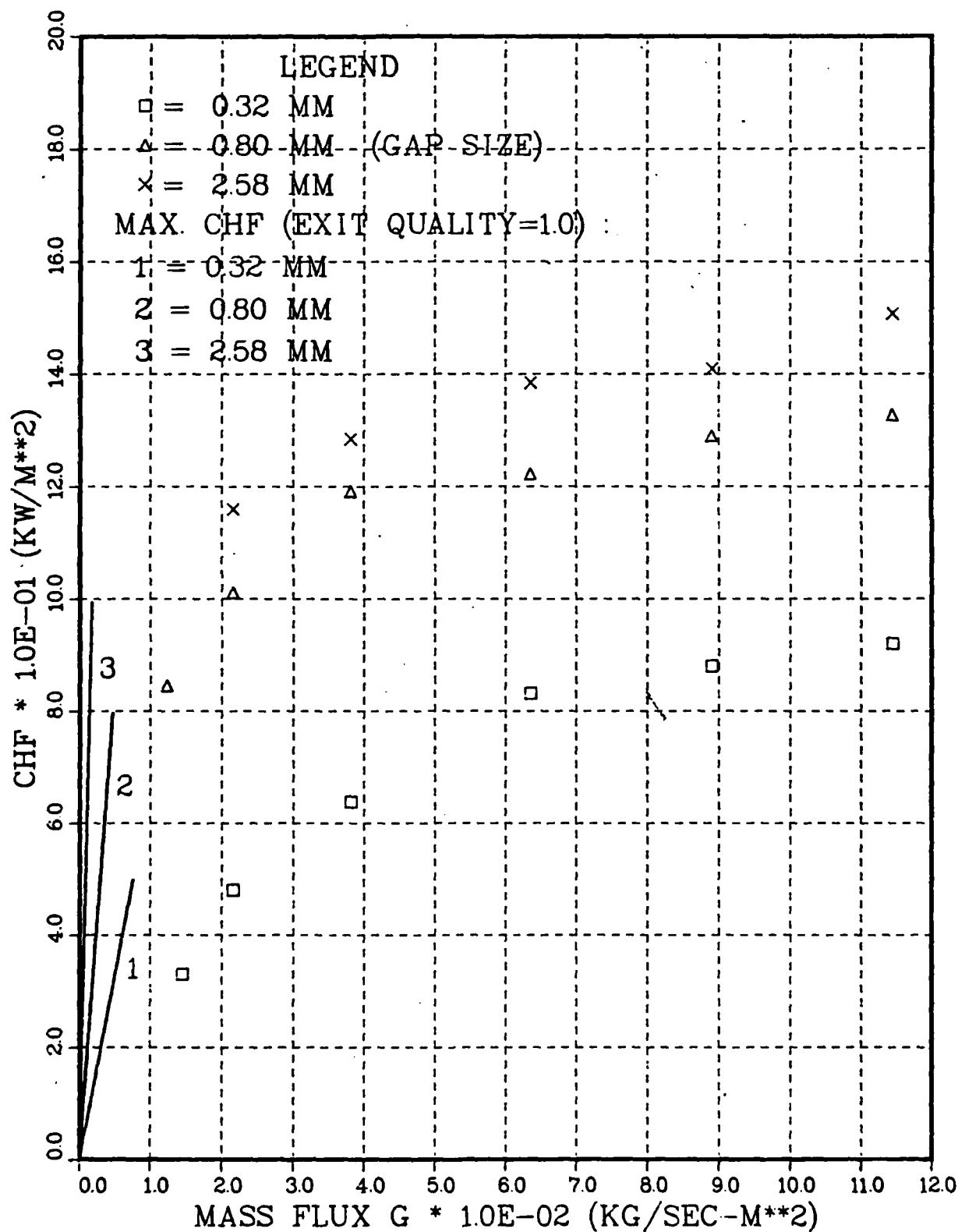


VIEW A

Fig 4

Fig. 5

CHF .VS. MASS FLUX



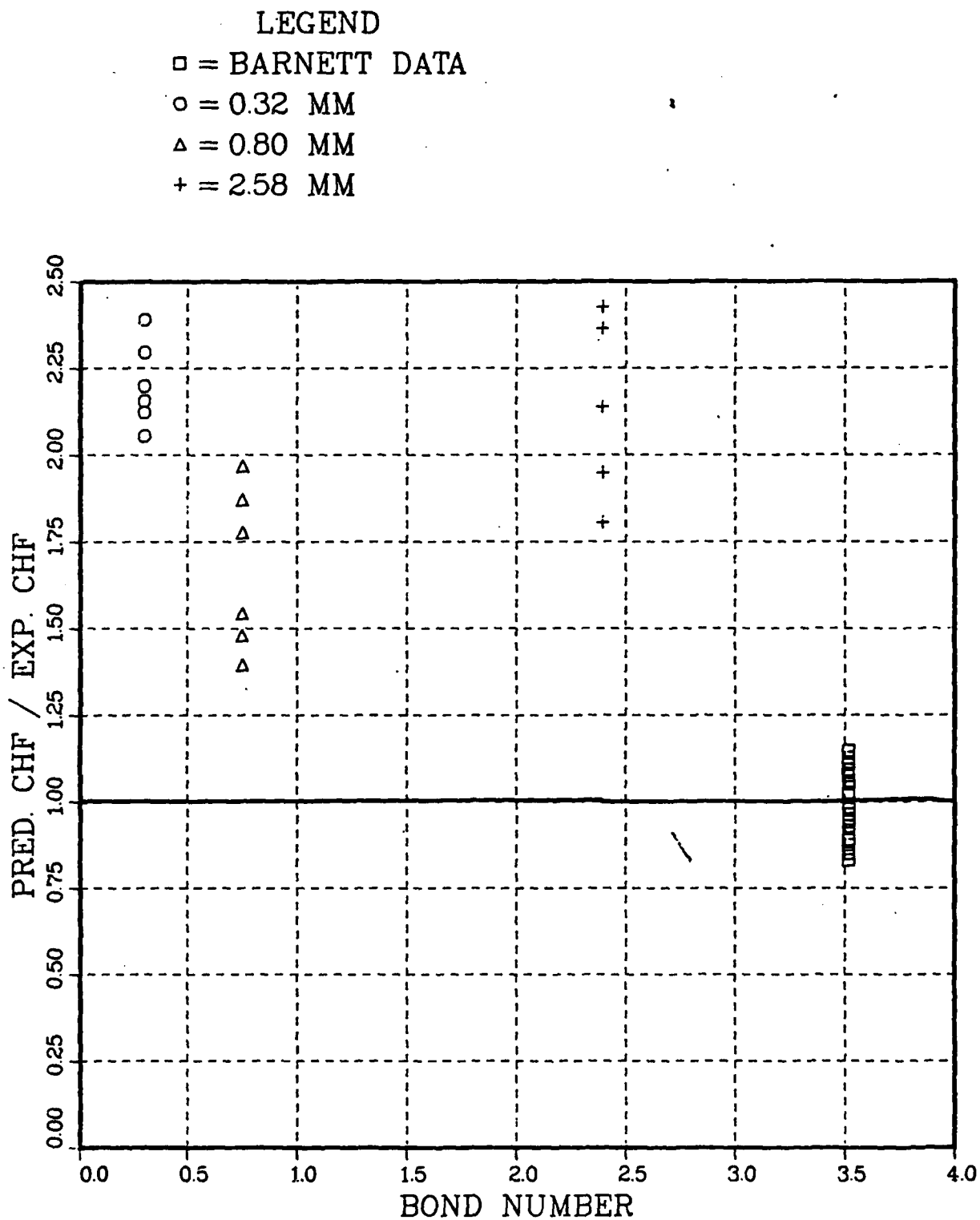


Fig. 6

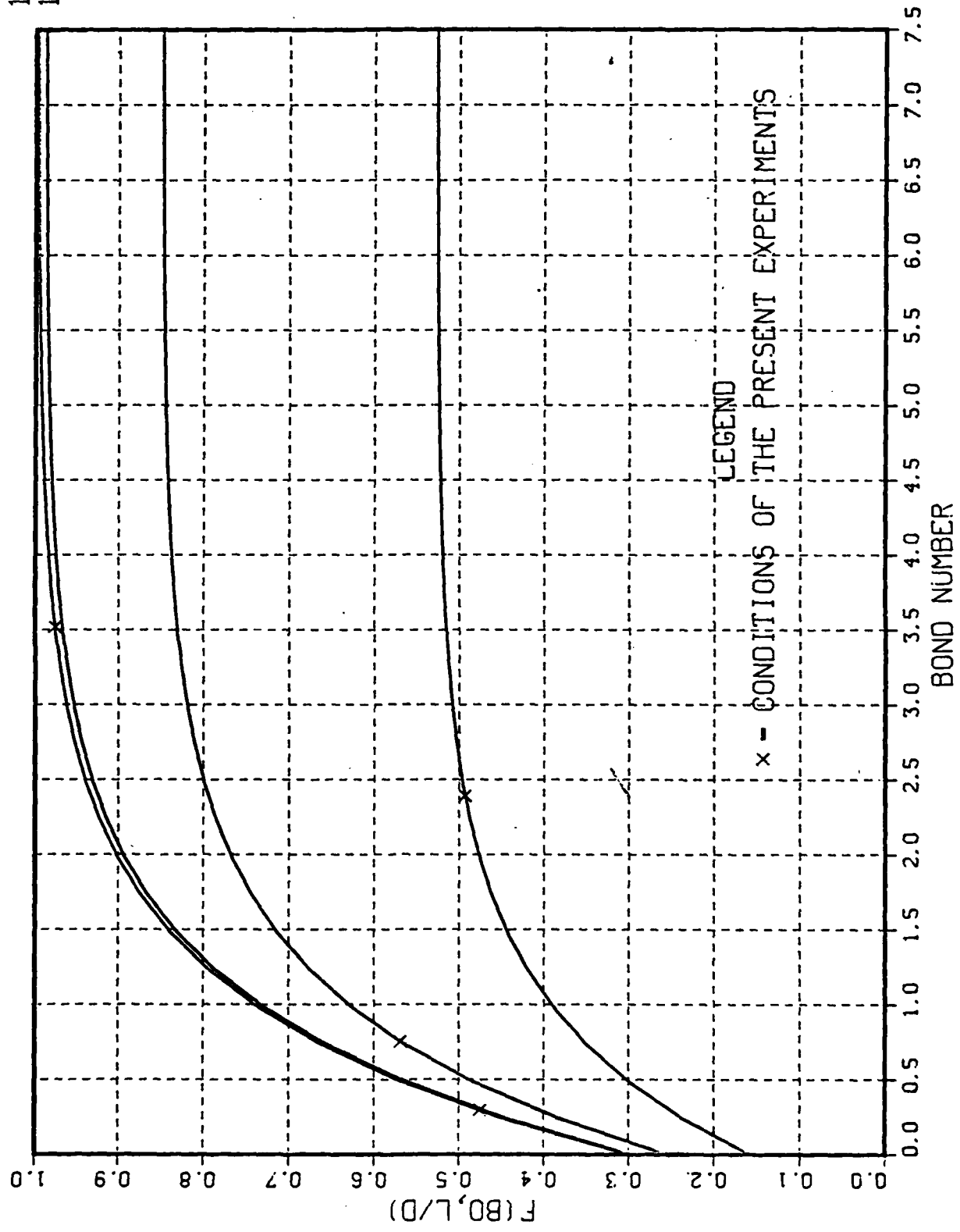
Fig.7 THE MODIFIED FUNCTION F

L/D

161.4
119.1

47.6

14.8



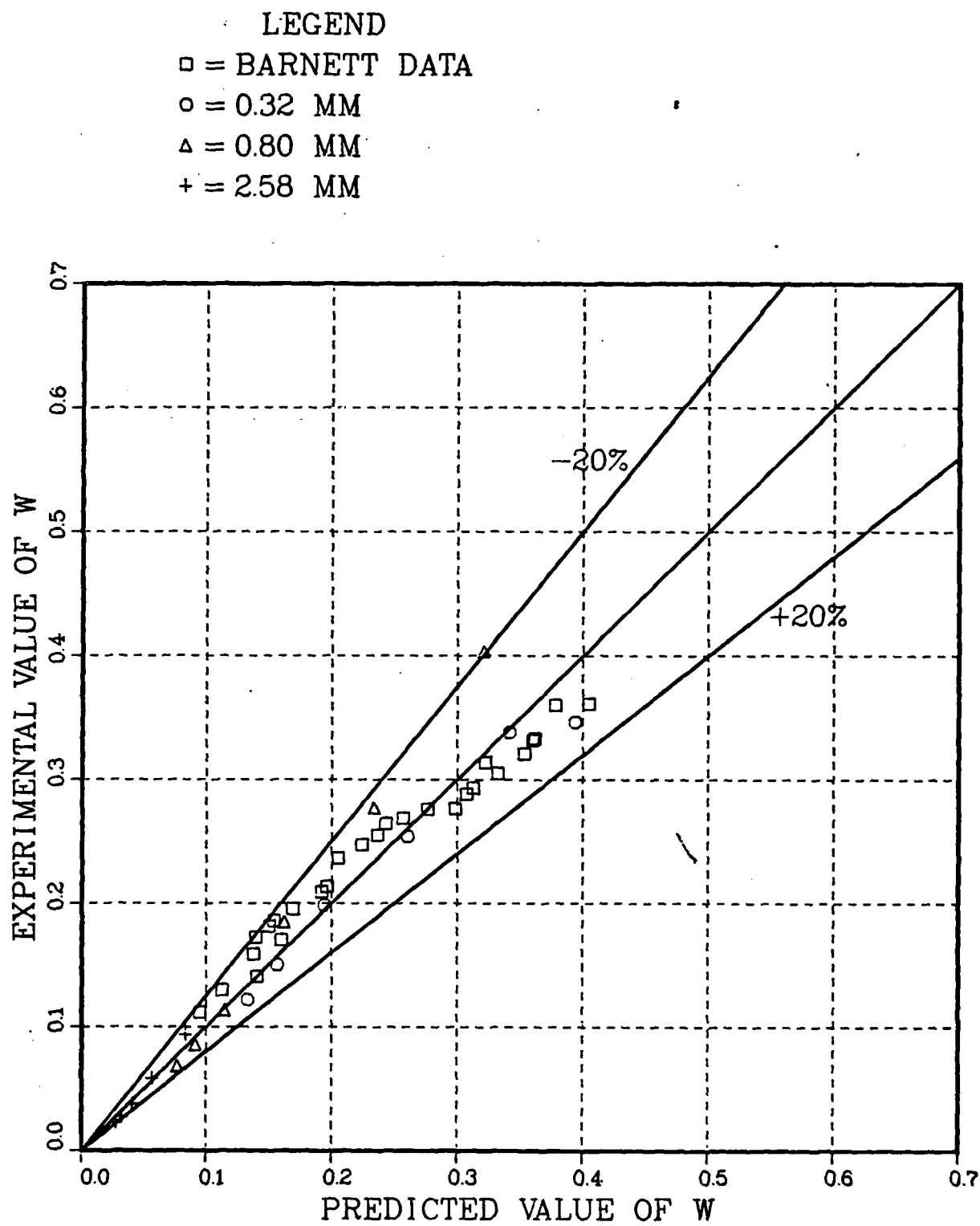


Fig. 8

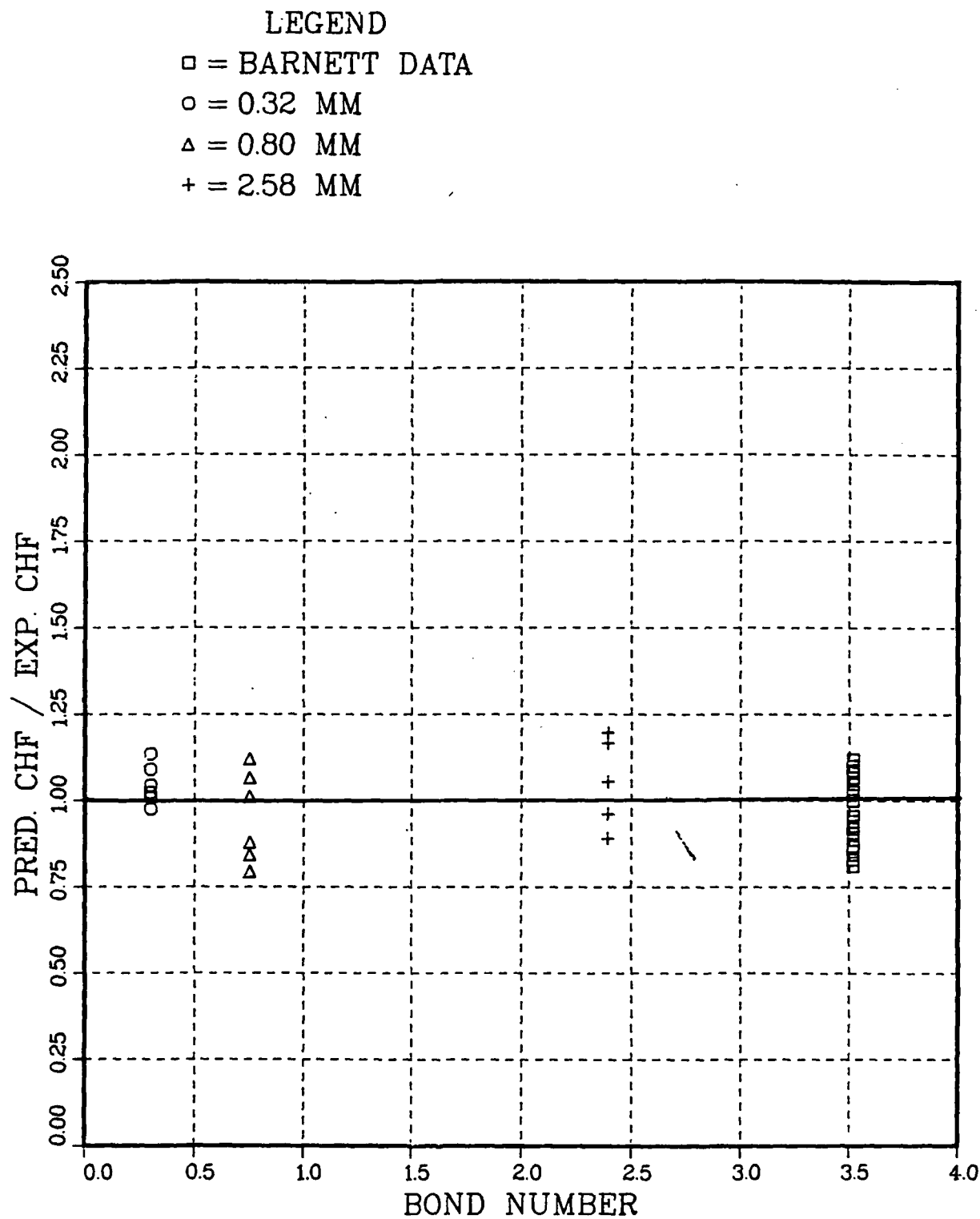


Fig. 9

CHAPTER 2
HEAT TRANSFER
OF
FORCED CONVECTIVE BOILING IN CONFINED SPACES

NOMENCLATURE

B_l	Boiling number, $q/(G\lambda)$
Bo	Bond number for the gap, defined in equation (4)
CHF	Critical heat flux
D	Hydraulic equivalent diameter = $4 \times \text{flow area} / \text{wetted perimeter}$
d_i	Outer diameter of the heated tube
d_o	Inner diameter of the quartz, $d_o = d_i + 2\delta$
G	Mass flux
g	Acceleration of gravity
H_{in}	Enthalpy of liquid at inlet
H_l	Enthalpy of saturated liquid
ΔH_{in}	$H_l - H_{in}$
h	Heat transfer coefficient
k	Liquid conductivity
Nu	Nusselt number, hD/k
P	System pressure
Pr	Prandtl number
q	Heat flux
q_B	Heat flux obtained from fully developed boiling correlation (3)
q_{FC}	Heat flux obtained from the correlation of single phase forced convection (1)

Re	Liquid Reynolds number, GD/μ_l
T	Temperature
T_{ib}	Temperature at the incipient boiling point
T_{sat}	Saturated temperature of the fluid
ΔT_{sat}	$T - T_{sat}$
$\Delta T_{sat,ib}$	$T_{ib} - T_{sat}$

GREEK SYMBOLS

ρ_l	Density of liquid phase
ρ_g	Density of vapor phase
μ_l	Viscosity of liquid phase
λ	Latent heat of vaporization
δ	Gap thickness
σ	Surface tension of liquid phase

HEAT TRANSFER OF FORCED CONVECTIVE BOILING IN CONFINED SPACES

INTRODUCTION

Heat transfer in nucleate boiling is the most efficient means of energy transfer that we use nowadays in thermal processes, so it receives most of the attention devoted to studies on boiling heat transfer. The behavior of nucleate boiling has been widely discussed over the past several decades, and numerous papers on this subject were indicated in the literature survey of boiling by Rohsenow & Hartnett [1] and Cole [2].

For the study of boiling phenomena, Ishibashi and Nishikawa [3] observed the saturated pool boiling heat transfer mechanism in a vertical annulus with a narrow space, and they proved that there is a coalesced bubble region having remarkably different characteristics from the isolated bubble region, the heat transfer characteristics of which have already been confirmed by many researchers. They also demonstrated that the heat transfer characteristics are closely associated with the boiling pattern in the narrow space. Akoi [4] conducted a series of experiments for pool boiling in vertical annuli with an electrically heated inner tube. For both ends open tests, he obtained that the boiling curve shifts toward the left side as the gap size is decreased, i.e., the heat transfer rate increases by reducing the gap size. The similar results were also reported by Ishibashi et al. [3]. Yao and Chang [5] presented a series of systematic investigations of pool boiling heat transfer in vertical narrow annuli with closed bottoms. They found that the bond number

is important to characterize the boiling behavior into three different boiling regimes.

To determine the shape of the heat flux curve in local boiling, Bjorge et al. [6] postulated a modified method of superposition for correlating forced convection boiling heat transfer data of water in tubes, and the method may be extended for use with other fluids by determining the special parameter which applies to each fluid.

Although the heat transfer of nucleate boiling in smooth annuli with forced convection has been studied by many researchers [7,8,9], until now the knowledge of nucleate boiling heat transfer in confined spaces for various gap sizes and convective mass fluxes has not been adequate to permit even a reasonable calculation of heat flux. Better predictive results can only follow from a better understanding of the physical mechanism of flow boiling. Due to this reason, the upward flow of Freon-113 in a vertical annulus with inner heating wall is considered in the present work. Because of the lack of sufficient experimental information in this field, it is very important to conduct a systematic study of the governing mechanisms and observe the effects of the boiling space confinement and mass flux on forced boiling behavior.

Therefore, the objectives of the present investigation are to obtain a systematic experimental data base for the forced boiling heat transfer behavior in confined spaces; and then to observe the effects of gap size and mass flux on boiling phenomena through visualization.

EXPERIMENTAL APPARATUS AND PROCEDURE

Several vertical, concentric narrow annular test sections which consist of electrically heated inner tubes and insulated quartz outer cylinders are used in the present experimental study. The annulus between the heated tube and the quartz cylinder simulates the gap between the tube and the support-plate in conventional steam generators and heat exchangers.

In the experiments, Freon-113 is used as the working fluid at a pressure slightly higher than atmospheric pressure. After any change of operation condition, the free adjustable parameters (e.g., P , G , ΔH_{in}) are kept at constant values for at least 5 minutes before measurements are taken. At that moment all parameters have reached steady states.

A pair of traversable thermocouples are used to measure the inside wall temperature of the heated tube. Two J-type, stainless steel sheathed, ungrounded thermocouples of 0.81 mm diameter are pressed against the inner-wall by plate-springs with a force of 5.87 newtons. The thermocouples are usually located 6.35 mm below the top opening of the narrow annulus to detect the early critical heat flux; and to observe the forced boiling heat transfer behavior. The detailed experimental apparatus and procedure have already described in the previous chapter.

RESULTS AND DISCUSSION

The test conditions including the range of Reynolds number in the present experiments are listed in Table 1. The critical heat flux results have been discussed in the previous chapter. Therefore, the experimental results in this part will be presented in three different sections. They are (1) characteristics of the boiling curves ; (2) effects of mass flux and gap size ; and (3) visual observation.

Characteristics of the Boiling Curves

The boiling curves for different gap sizes are plotted in Figures 1, 2, and 3 respectively. Since the liquid at the inlet of the test section is generally subcooled, at low heat fluxes the heat is transferred by single-phase forced convection with no boiling occurs within the confined spaces. When the heat flux is increased to a higher level to initiate the nucleation, bubbles appear at the downstream over the upper half surface of the heating tube. A remarkable hysteresis is usually observed.

With further increases of heat flux, both the mass fluxes and the gap sizes influence the boiling phenomena. At higher heat fluxes, nucleation is initiated at locations of the heating surface which are more close to the inlet of the test section. The boiling is rather fully developed over the majority of the heated area. At this condition, the effect of mass flux to the boiling heat transfer has diminished, but the effect of gap size is still significant.

Single-Phase Forced Convection

The range of the Reynolds number for different gap sizes in the experiments is shown in the Table 1. Except the case of the smallest gap, where the flow is laminar, the flow covers the range from laminar flow to turbulent flow. The evaluation of heat transfer coefficient for Reynolds number less than 2000 follows the laminar flow, thermal-entry length solution for annulus which is indicated in the text book of Kays and Crawford [11]. The corresponding heat transfer coefficients for Reynolds number larger than 2000 can be calculated from the existing equation for the concentric circular annulus as indicated in [10]. That is

$$Nu = 0.023 Re^{0.8} Pr^{0.4} (d_o/d_i)^{0.5} \quad (1)$$

where

d_o = inner diameter of the quartz = $d_i + 2\delta$

d_i = outer diameter of the heated tube

δ = gap thickness

Some calculated results are shown in Figures 1-3 together with the data. In Figures 1-3, the experimental results usually are higher than the theoretical results which are obtained from equation (1) and the reference [11]. The reason may be due to the roughness effect of the heated surface [10]; the heat loss which was neglected in the experiments; and the measurement error for wall temperature. Although there is a difference between the experimental

data and the calculated results, the general trend of heat transfer in the experiments is consistent with the theoretical predictions.

Hysteresis

The boiling hysteresis occurs at the transition between the single phase and the nucleate boiling. The boiling hysteresis is observed at increasing heat flux but not at decreasing heat flux. The overshoot of the wall superheat happens before the inception of the boiling. As shown in Figures 1-3, the hysteresis does not occur in the experiments when the mass flux is equal to 1144.9 kg/m²sec for all the three gap sizes.

Heat Transfer of Local Nucleate Boiling

Convective boiling heat transfer data have been correlated by Bjorge et al. [6]. In this correlation the flow boiling heat flux in tubes is calculated from the fully developed boiling heat flux and the single-phase forced convection heat flux in the form of

$$q = \{q_{FC}^2 + q_B^2 [1 - (\frac{\Delta T_{sat,ib}}{\Delta T_{sat}})^3]^2\}^{1/2} \quad (2)$$

for subcooled and low quality flow.

The fully developed boiling heat flux can be expressed in the following form the present data :

$$q_B = 0.27 (\Delta T_{sat})^2 \quad (3)$$

The proposed formulation of equation (2) has been compared with the present forced convection boiling data in narrow annuli. The evaluated heat transfer coefficient of single-phase forced convection for 2.58 mm gap size is 1.31 kW/m²°C and 0.35 kW/m²°C for the mass flux of 1144.9 kg/m²sec and 216.0 kg/m²sec respectively. The predictions of the boiling curve for the experiment of 2.58 mm gap size with the mass fluxes 1144.9 and 216.0 kg/m²sec are also shown in Figures 4 and 8 respectively.

Fully Developed Flow Boiling

Tong [12] and Lemmert et al. [13] postulated that no heat is transferred by forced convection in the fully developed region. This conclusion was based upon the fact that the available data of fully developed boiling indicate neither the significant effect of subcooling nor the significant effect of mass flux on the boiling heat transfer. Collier [14] concluded that at forced convective condition the fully developed region of the boiling curve had generally been assumed to coincide with the extrapolation of the pool boiling curve. Generally, this assumption appears to be reasonable for low velocity flow. Experiments carried out by Bergles and Rohsenow [15] were designed with the object of directly comparing data for pool boiling and forced convection boiling. They concluded that forced convection boiling

cannot be considered an extrapolation of pool boiling for their experimental data [15]. However, it would appear that the form of the equations suitable for the correlation of pool boiling data is suitable for the representation of the data of forced convective, fully developed, subcooled boiling. The values of the slope and intercept (i.e. n and a of $\Delta t_{sat} = a \cdot q^n$) will, of course, need to be altered from the values obtained from pool boiling.

According to the above conclusion, the correlation of fully developed boiling heat flux in the present work can be obtained from the present experimental data , its form is expressed as equation (3) and shown in Figures 1 - 8. The experimental results for open tube pool boiling by Yao and Chang [5] are also presented in the Figures.

Effects of Mass Flux And Gap Size

Effect of Mass Flux

The wall heat flux versus the wall temperature of the heated tube is plotted in Figure 1 for the experiments of 2.58 mm gap size at various mass fluxes (216.0, 381.6, 636.0, 890.4, and 1144.9 kg/m²sec respectively). Similar boiling curves are presented in Figures 2-3 for the cases of gap sizes 0.80 and 0.32 mm at the same mass fluxes.

It is interesting to compare the various curves in a same Figure. At single phase forced convection, the trend of the data is consistent with the

theoretical prediction that the heat transfer coefficient increases with the increasing mass flux. When the heat flux is further increased the inception of boiling occurs and the wall superheat suddenly reduces. This hysteresis is generally observed. The lower the mass flux the more the incipient boiling superheat. At the highest mass flux in the experiments (1144.9 kg/m²sec), the boiling inception superheat is not observed.

At intermediate heat flux the convective boiling heat transfer is affected by the mass flux. The higher the mass flux the higher the heat flux at a same wall superheat. In other words, the effect of the flow still exists. At the high heat flux conditions, the boiling is fully developed. There is no significant effect of the mass flux on the boiling curves for large gap sizes of 2.58 and 0.80 mm. This is consistent with the observations by various previous researchers [13,16,17]. However, there is still significant effect of mass flux on the boiling curves for the case of 0.32 mm gap size in Figure 3. The reason for this contradiction to the large gap cases might be due to the thin film evaporation which causes dryout to occur at lower CHF levels than conventional large gap cases.

Effect of Gap Size

The size of the gap affects the behavior and the heat transfer of boiling in annuli. The boiling curves for various gap sizes at specific mass fluxes are shown in Figures 4 to 8 in the order of decreasing mass flux. Generally, with the increase of the gap size the boiling curve asymptotically approaches to the conventional fully developed boiling curve. Furthermore, it is observed that

when the gap of the flow channel is very small the boiling heat transfer at the same mass flux is increased with respect to the conventional results of tubes or annuli with a large flow channel. Increases of the convective boiling heat transfer in very narrow gaps are attributed to thin film evaporation under the deformed bubbles. A similar trend has been reported by Ishibashi et al. [3] and Akoi [4] for the pool boiling in vertical narrow annuli.

Visual Observation

In the present study, the boiling phenomena have been observed through the transparent quartz shroud. As observed from the photographs of the boiling at the condition of narrow gaps, the bubbles have been severely squeezed as the shape of pancakes between the walls. A non-dimensional parameter called Bond number can be used to relate the gap size and the capillary constant as

$$Bo = \delta / [\sigma / g(\rho_l - \rho_g)]^{1/2} \quad (4)$$

In some sense, the Bond number can also be related as the ratio of the gap size and the bubble departure diameter in the conventional pool boiling. Furthermore, the previous study of Yao and Chang [5] on the pool boiling in narrow gaps indicated that the boiling regimes can be related with the Bond number of the system at low heat flux. Therefore, the Bond number will be used to classify the boiling regimes for the effect of the gap size. The three

boiling regimes in the confined space have been defined. They are non-deformed bubbles, isolated deformed bubbles, and coalesced deformed bubbles. The boiling regimes are dependent of the gap dimension which can be represented as the Bond number of the gap.

For the experiments with Bond number 2.394 (gap thickness 2.58 mm) the boiling phenomena at constant mass flux but different heat flux are shown in Figure 9. At low heat flux, many small non-deformed spherical bubbles are generated from the heating surface. When the heat flux gradually increases up to CHF, no significant change of the bubble shape is apparent except the bubbles become slightly deformed in shape.

For the experiments with Bond number 0.754 (gap thickness 0.80 mm) the boiling phenomena at constant mass flux but different heat flux are shown in Figure 10. Since the gap size is reduced, the bubbles start with spherical shape then are deformed as individual pancakes. With the further growth of the deformed bubbles they may merge together as coalesced deformed bubbles.

For the experiments with Bond number 0.300 (gap thickness 0.32 mm) the boiling phenomena are presented in Figure 11 for constant mass flux but different heat flux. Since the gap is very small, all the bubbles are highly deformed in the narrow annulus. Isolated deformed bubbles are generated within the confined space. When heat flux is increased many isolated deformed bubbles merge as coalesced bubbles.

The forced convective boiling behavior in confined spaces can be classified into three regimes in terms of the gap Bond number, which

characterizes the effect of geometric confinement, and the Boiling number, which is defined as $B_f = q/G\lambda$. The boiling regimes of the present study are expressed in terms of Bo and B_f in Table 2.

The non-deformed bubble regime occurs when the Bond number is larger than about 1.0 and at low heat flux condition. The bubbles may be slightly deformed at high heat flux condition when the Bond number is above 1.0. The isolated deformed bubble usually occurs when the Bond number is less than unity. The coalesced deformed bubble regime exists at high heat flux condition when the Bond number is less than 1.0, or even at low heat flux condition when the Bond number is very small. The observations in the present work for convective boiling phenomena are qualitatively consistent with the observation in the pool boiling by Yao and Chang [5]. In that work the Bond number of unity is regarded as the criterion for classifying the boiling regimes, too. Therefore, it is reasonable to use the Bond number to classify the boiling regime for both the pool boiling and the convective boiling in confined spaces.

CONCLUSIONS

The forced convective boiling heat transfer in confined spaces has been observed for various gap sizes and mass fluxes. Based on the investigation of this study, the following conclusions on the nucleate boiling heat transfer in confined spaces are reached :

1. In the local boiling region, the boiling curves for three gap sizes

are affected by the mass flux. The higher the mass flux the higher the heat flux at a same wall superheat. When the heat flux is further increased, the boiling will become fully developed. There is no significant effect of the mass flux on the boiling curves for large gap sizes of 2.58 and 0.80 mm, but the effect of mass flux on the boiling curve for very small gap 0.30mm is still existed.

2. When the gap size decreases, the boiling heat transfer at the same mass flux is increased due to the effect of thin film evaporation. With the increase of gap size the boiling curve asymptotically approaches to the conventional fully developed boiling curve.
3. The hysteresis effects are observed in the transition region between single-phase convection and nucleate boiling at different mass-flux measurements. When heat flux is increasing, it does not occur in all experiments, and no overshoot phenomenon has been detected as the heat flux decreases.
4. The convective boiling phenomena in confined spaces can be classified into three boiling regimes : non-deformed, isolated deformed, and coalesced deformed bubble regimes. The boiling regimes can be identified in terms of Bond number and Boiling number of the system.

REFERENCES

1. W. M. Rohsenow and J. P. Hartnett, "Handbook of Heat Transfer," Section 13 : Boiling, McGraw-Hill, New York, 1973.
2. Robert Cole, "Nucleate-Boiling Heat Transfer, A General Survey," (III) Nucleate Boiling, *Boiling Phenomena*, Vol. 1, pp.155, Hemisphere Publishing Corporation, 1979.
3. E. Ishibashi and K. Nishikawa, "Saturated Boiling Heat Transfer in Narrow Spaces," *Int. J. Heat Mass Transfer*, Vol. 12, pp.863, 1969.
4. S. Akoi, "Boiling Heat Transfer in a Narrow Gap (Electrical Heating)," Chapter 5.
5. S. C. Yao and Y. Chang, "Pool Boiling Heat Transfer in Confined Spaces," Submitted to *Int. J. Heat Transfer*, March 1982.
6. Robert W. Bjorge, Garry R. Hall and Warren M. Rohsenow, "Correlation of Forced Convection Boiling Heat Transfer Data," *Int. J. Heat Mass Transfer*, Vol. 25, No. 6, pp.753, 1982.
7. L. Bernath and W. Begell, "Forced Convection Local Boiling Heat Transfer in Narrow Annuli," *Heat Transfer-Chicago, Chemical Eng. Prog. Symp. Series*, Vol. 55, No. 29, pp. 59, 1959.

8. J. R. S. Thom, W. M. Walker, T. A. Fallon, and G. F. S. Reising, "Boiling in Subcooled Water during Flow up Heated Tubes or Annuli," Symp. Boiling Heat Transfer in Steam Generation Units and Heat Exchangers, Inst. Mech. Eng. (London), Manchester, England, Paper 6, September 15-16, 1965.
9. H. Lung, K. Latsch, and H. Rampf, "Boiling Heat Transfer to Subcooled Water in Turbulent Annular Flow," *Heat transfer in Boiling*, Hemisphere Publishing Corporation, Washington, pp.219, 1977.
10. V.S. Chirkin, and V. P. Iukin, "Critical Point in Heat Removal from Boiling Water Flowing through an Annular Gap," *Soviet Physics - Technical Physics*, No. 1, July-December, pp.1503, 1956.
11. W. M. Kays and M. E. Crawford, "Convective Heat Transfer and Mass Transfer," McGraw-Hill Book Company, 2nd Ed., pp.117, 1980.
12. L. S. Tong, "Boiling Heat Transfer and Two-Phase Flow," John Wiley & Sons, Inc., 1965.
13. M. Lemmert and J. M. Chawla, "Influence of Flow Velocity on Surface Boiling Heat Transfer Coefficient," *Heat Transfer in Boiling*, Hemisphere Publishing Corporation, Washington, pp.237, 1977.
14. John. G. Collier, "Convective Boiling and Condensation," McGraw-Hill, London, pp.156-163, 1972.

15. A. E. Bergles and W. M. Rohsenow, "The Determination of Forced Convection Surface Boiling Heat Transfer," Paper 63-HT-22, 6th National Heat Transfer Conference of the ASME-AIChE, Boston, August 11-14, 1963.
16. H. R. McKee and K. J. Bell, "Forced Convection Boiling from a Cylinder Normal to the Flow," Chemical Engineering Progress, Symposium Series, Vol. 65, No. 92, pp.222, 1969.
17. R. C. Bitter, "Heat Transfer from a Horizontal Tube with Transverse Flow of Evaporating Saturated R-11," International Institute of Refrigeration Commissions B-1, B-2 & E-1, Freudenstadt, Fed. Rep. of Germany, Supplement to International Institute of refrigeration Bulletin, pp.97, 1972.

Table 1. Range of Parameters for Operating Conditions

Working Fluid	Freon - 113		
Geometry	Vertical upflow in concentric annuli with internal heating		
System Pressure	0.132 MPa		
Saturation Temp.	55.6 ° C		
Material of heated tube	304 stainless steel seamless tube		
O. D. of heated tube	25.4 mm		
T/S Length	76.2 mm		
Inlet Subcooling	1.21 × 10 ⁴ J/kg		
Variable Parameters :			
Gap Size	0.32 mm	0.80 mm	2.58 mm
Reynolds Number Range	256 - 1359	646 - 3425	2052 - 10872

Table 2. Boiling Regimes in terms of Bo and B_i

Bo	I	II	III
0.300	None	$B_i \leq 2.4 \times 10^{-4}$	2.4×10^{-4} to 1.6×10^{-3}
0.754	$B_i \leq 6.0 \times 10^{-4}$	6.0×10^{-4} to 1.2×10^{-3}	1.2×10^{-3} to 4.9×10^{-3}
2.394*	$B_i \leq 2.0 \times 10^{-3}$	None	None

Where

- I : Non-deformed Bubble Regime
- II : Isolated Deformed Bubble Regime
- III : Coalesced Deformed Bubble Regime

* $2.0 \times 10^{-3} \leq B_i \leq 4.1 \times 10^{-3}$ in the case of $Bo=2.394$: Slightly Deformed Bubbles.

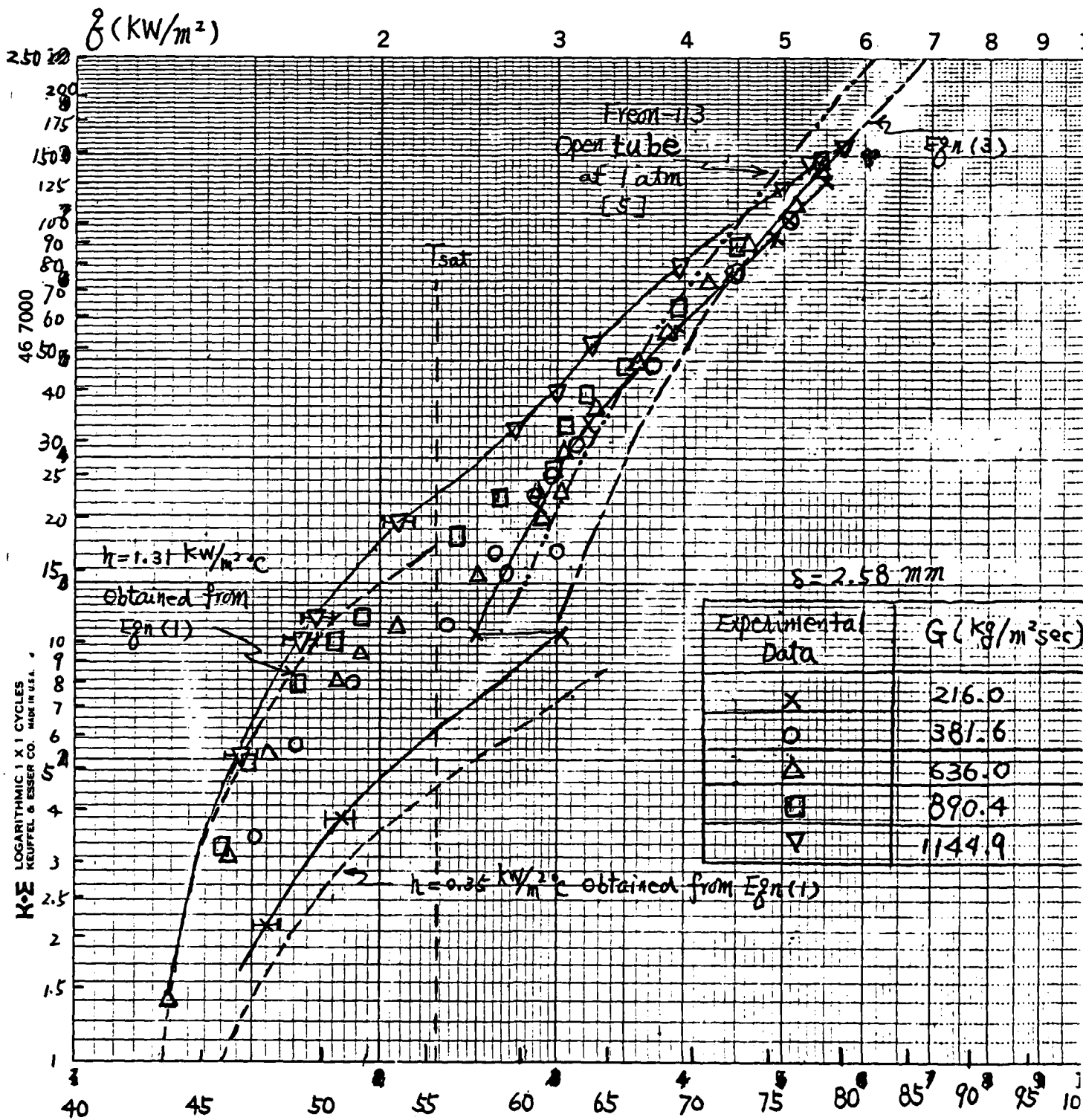


Fig. 1. Boiling Curves for Large Gap (2.58 mm)

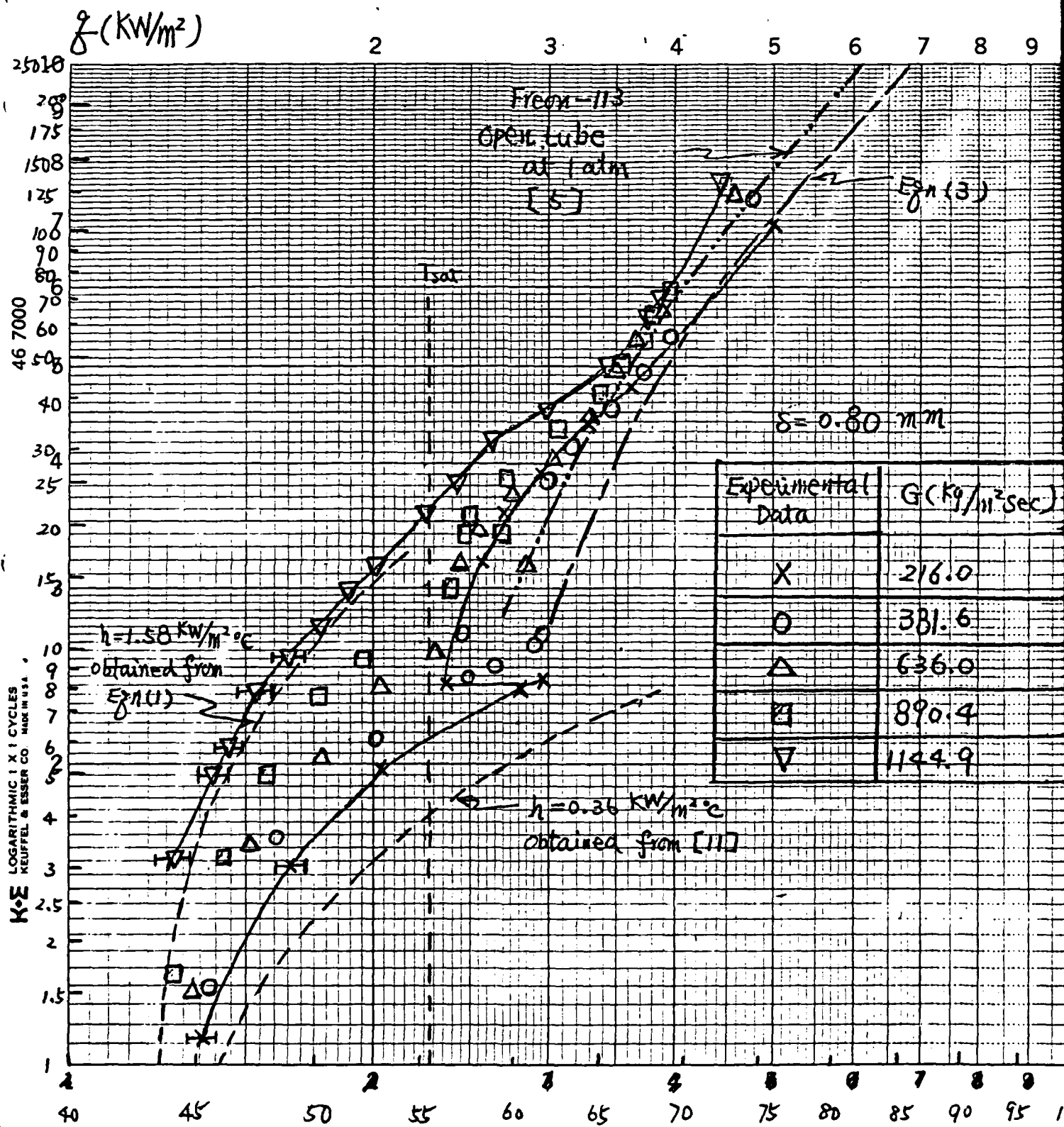


Fig. 2 Boiling Curves for Medium Gap (0.80 mm)

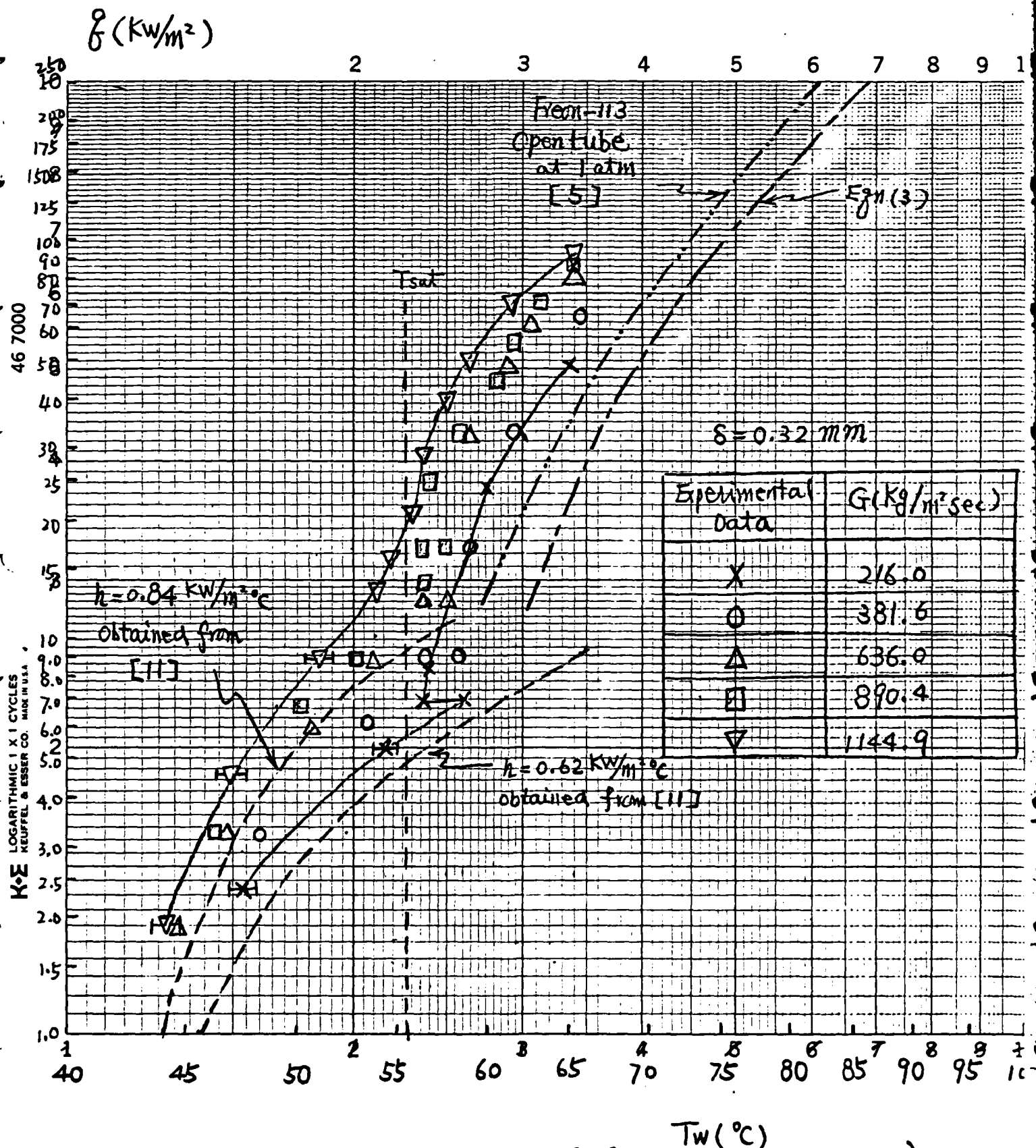


Fig. 3. Boiling Curves for Small Gap (0.32 mm)

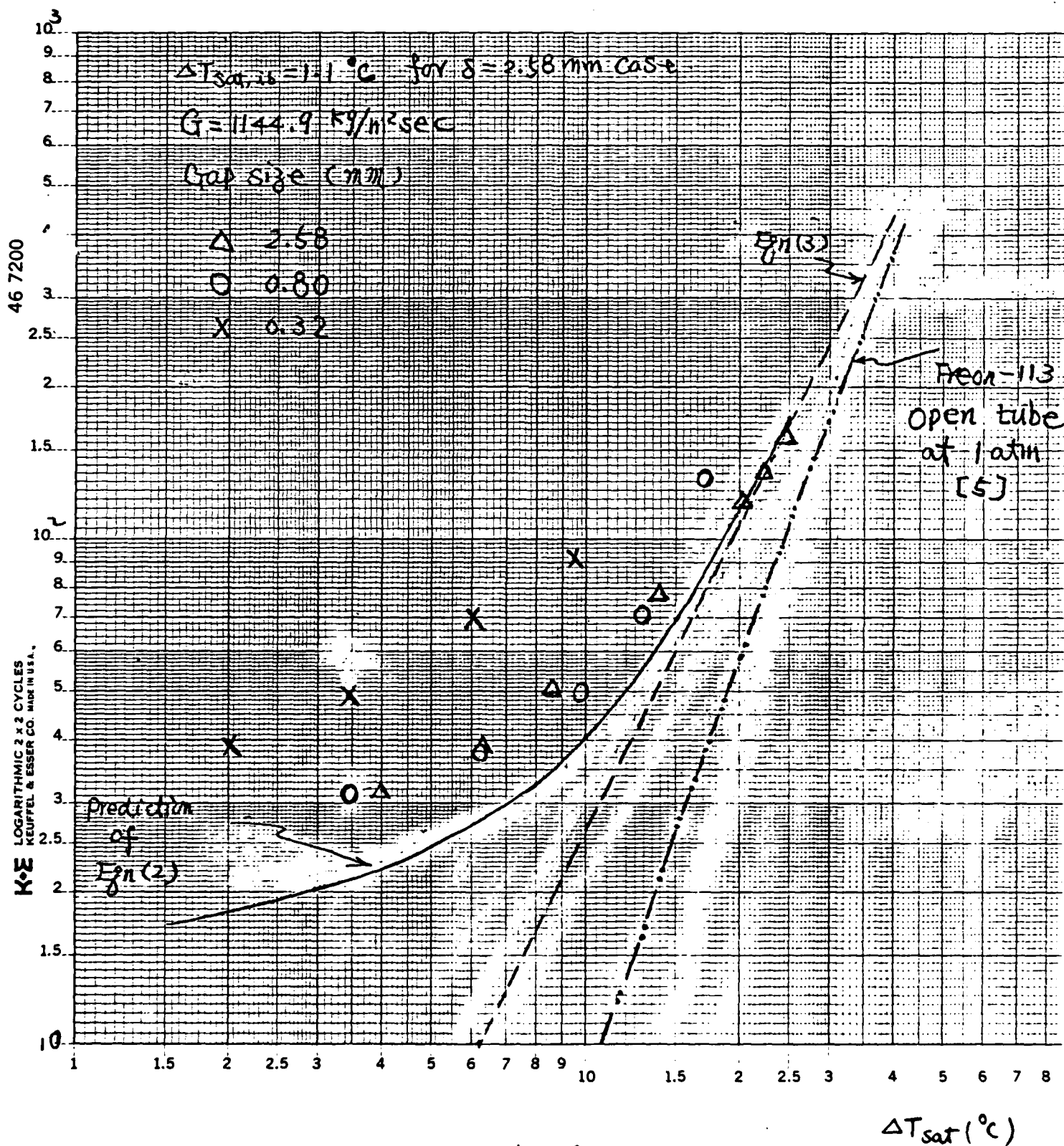


Fig. 4. Boiling Curves for Mass Flux $1145\text{ kg/m}^2\text{s}$

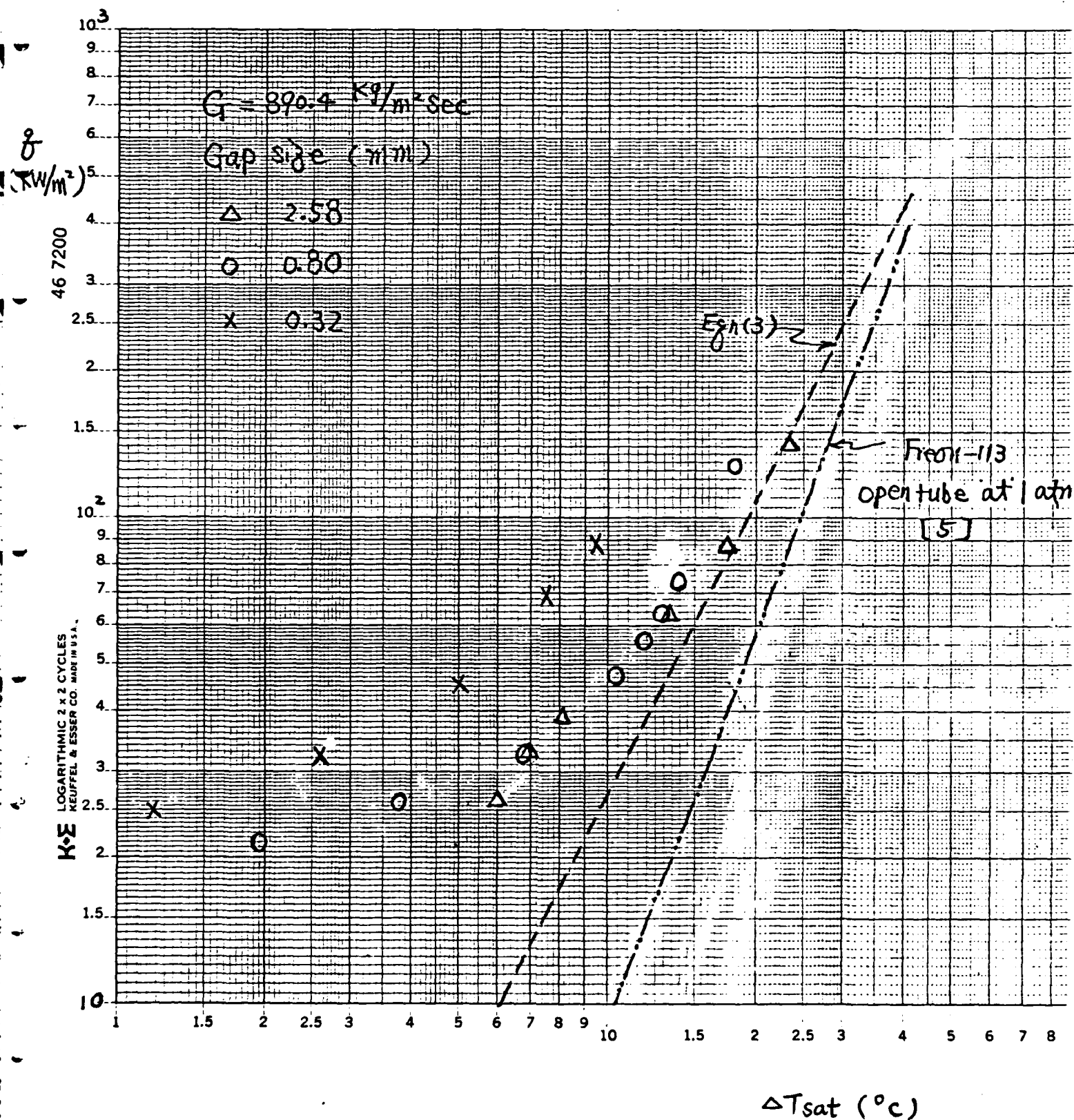


Fig. 5 Boiling Curves for Mass Flux 890 kg/m²s
 $\Delta T_{\text{sat}} (^{\circ}\text{C})$

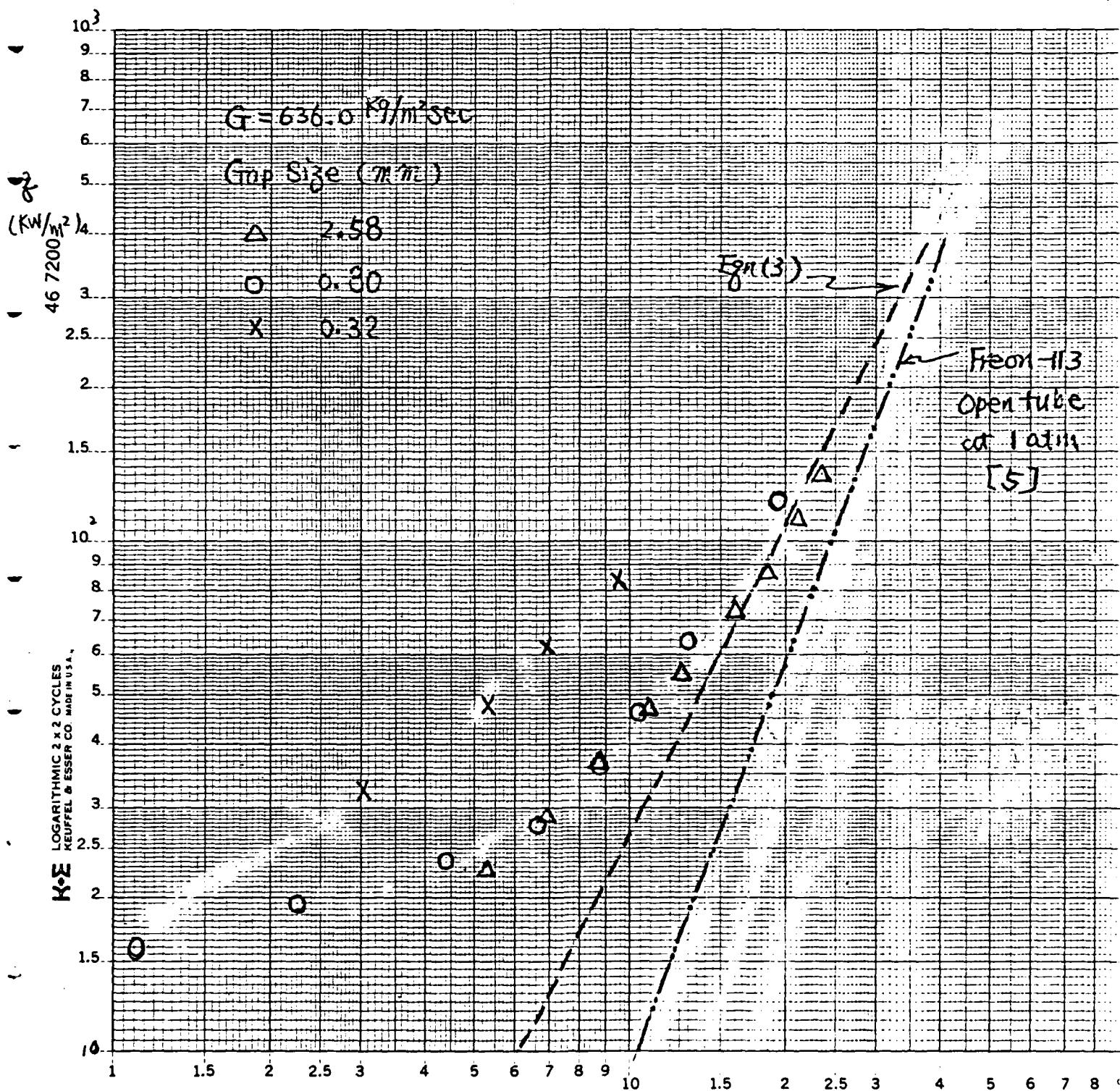


Fig. 6. Boiling Curves for Mass Flux 636 kg/m²s
 $\Delta T_{sat} (^\circ\text{C})$

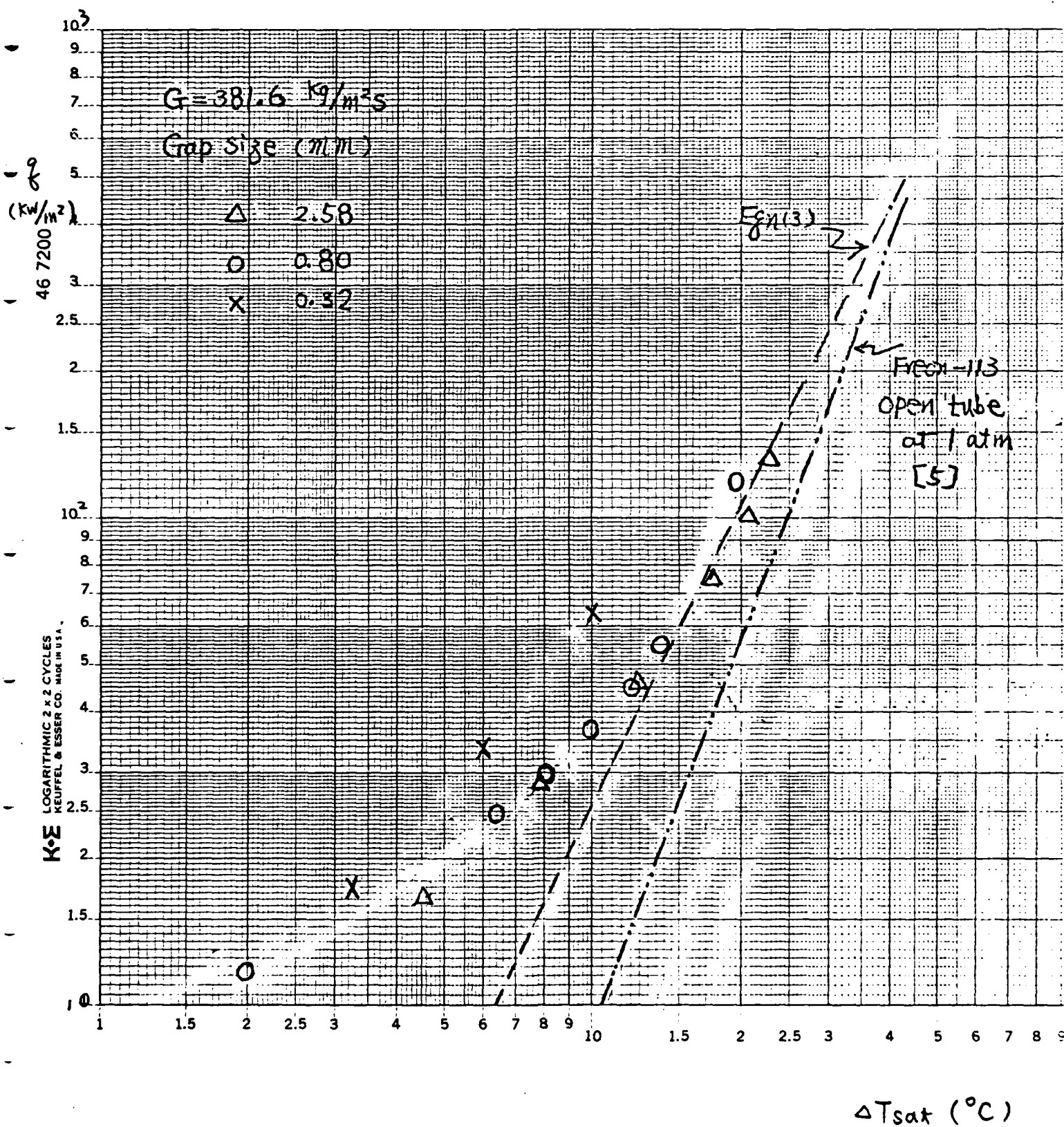


Fig. 7. Boiling Curves for Mass Flux 382 kg/m²s

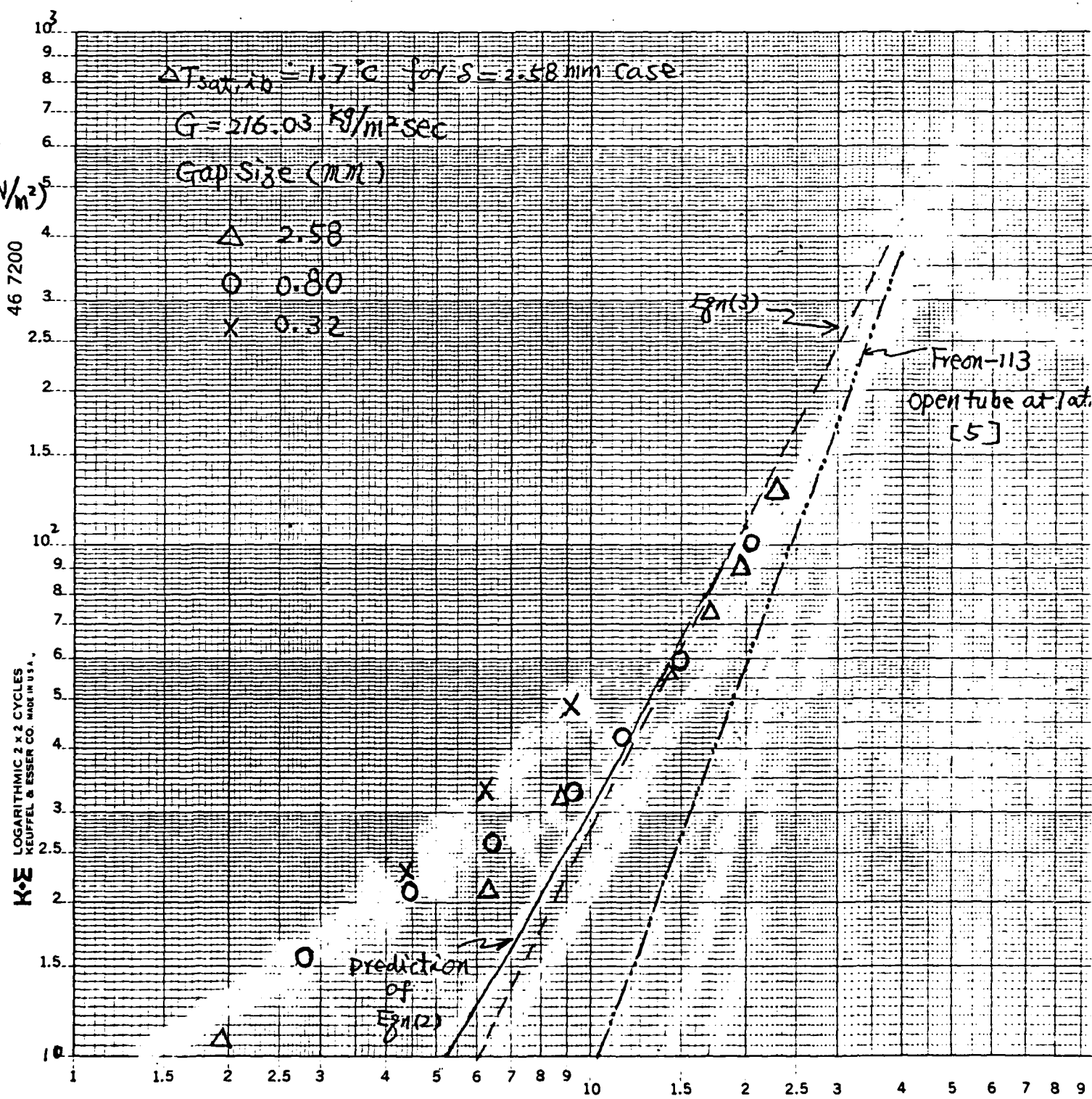


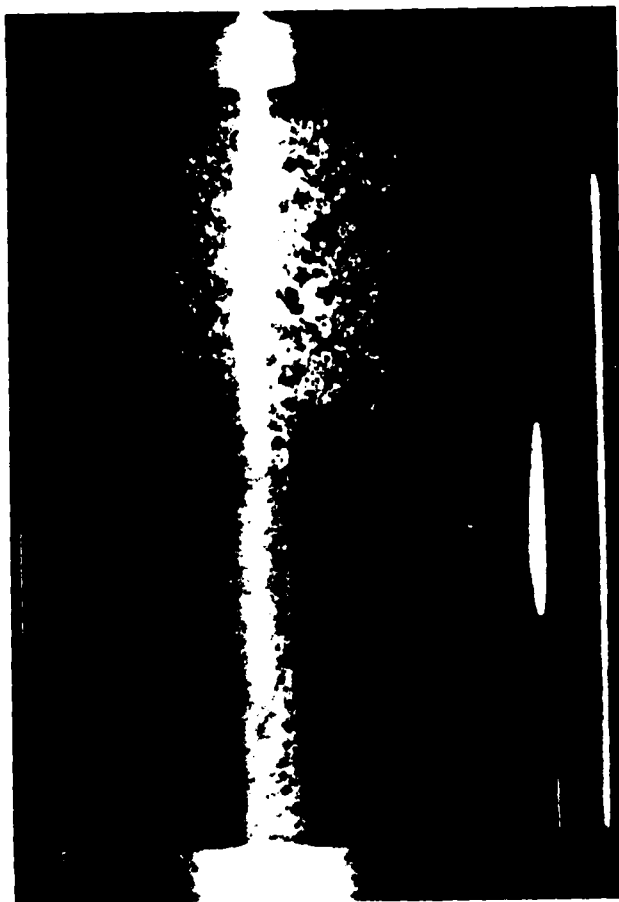
Fig 8. Boiling Curves for Mass Flux $216 \text{ kg/m}^2\text{-s}$ $\Delta T_{sat} (^\circ\text{C})$



26.0
 $\frac{KW}{m^2}$



47.7
 $\frac{KW}{m^2}$



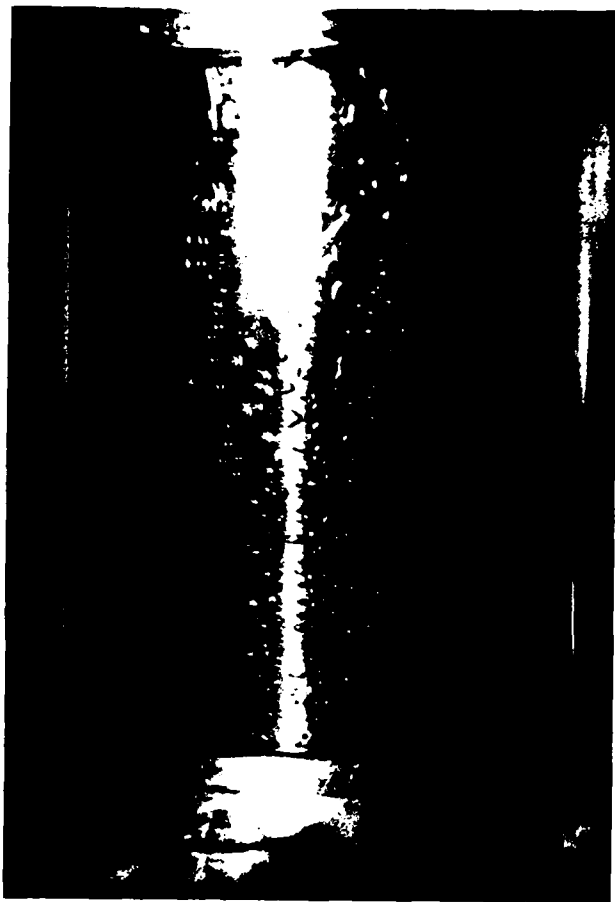
74.3
 $\frac{KW}{m^2}$



116.0
 $\frac{KW}{m^2}$
 (CHF)

$\Delta H_{lv} = 1.209 \times 10^4 \text{ J/kg}$

Fig. 9 Photographs of the Boiling for $S = 2.53 \text{ mm}$ $G = 216 \text{ kg/m}^2\text{-sec}$



26.0
 $\frac{5.11}{11.2}$



43.0
 $\frac{5.11}{11.2}$



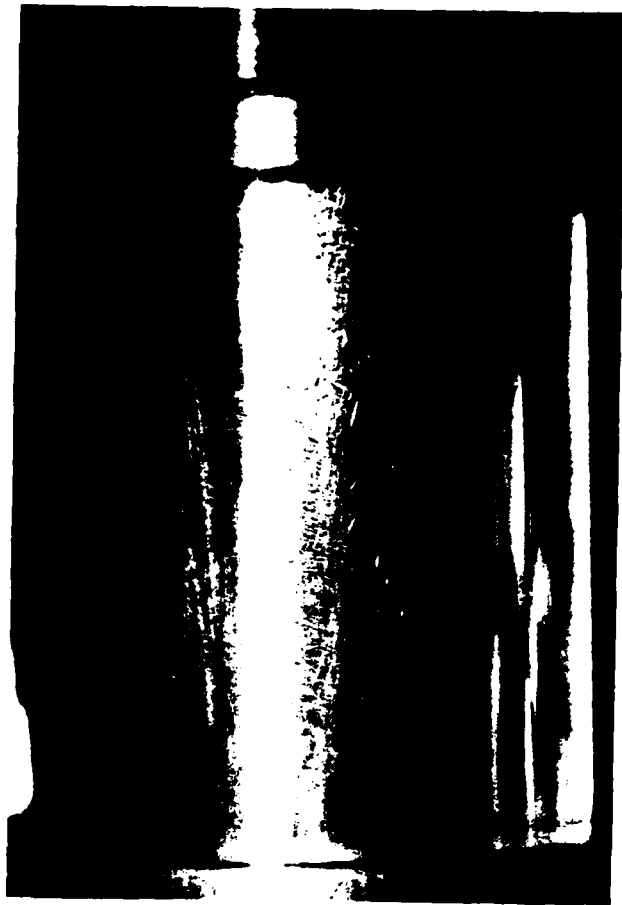
73.9
 $\frac{5.11}{11.2}$



101.2
 $\frac{5.11}{11.2}$
 0.045

• Page 6. Discharge of 4.5 PPM for

$24.1 = 1.269 \times 10^4$
 $2.5 = 2.5 \times 10^4$ $2.5 = 2.5 \times 10^4$



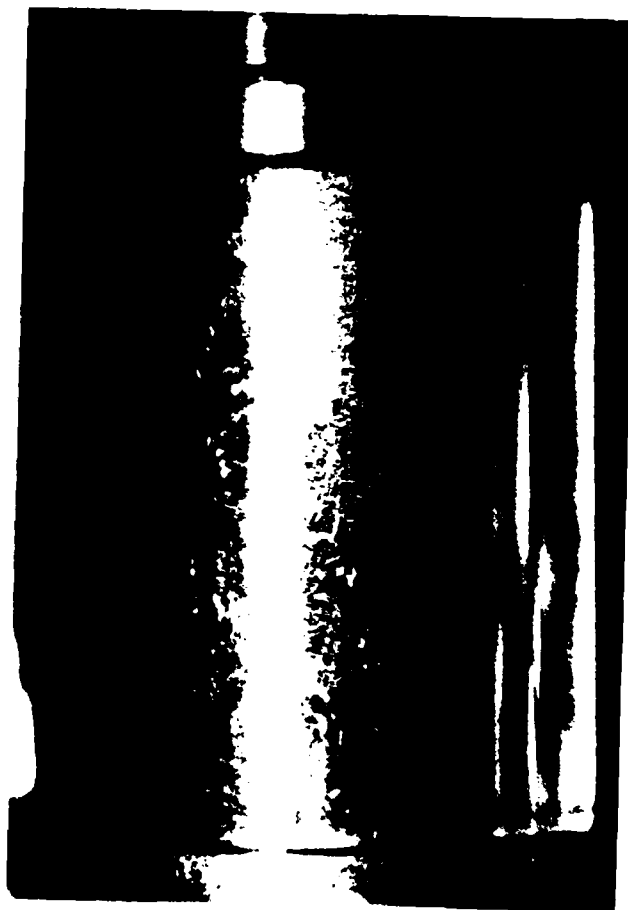
15.4
 $\frac{K_{II}}{m^2}$



21.6
 $\frac{K_{II}}{m^2}$



33.0
 $\frac{K_{II}}{m^2}$



42.1
 $\frac{K_{II}}{m^2}$

Fig. 1. Micrographs of the surface of

2H₂O = 1.217 x 10⁻⁴ m
S = 0.32 mm
C = 0.11 mm

CHAPTER 3

POOL BOILING IN HORIZONTAL ANNULAR CREVICES

POOL BOILING IN HORIZONTAL ANNULAR CREVICES

INTRODUCTION

The boiling in horizontal annular crevices is of great importance to the understanding and the design of tube to baffle supports in horizontal steam generators in avoiding the corrosive concentration induced corrosion. Saturated pool boiling for single tubes and horizontal plates has been extensively studied in recent years. However, knowledge on the effect of geometrical confinement to pool boiling heat transfer remains limited. Ishibashi and Nishikawa [1] studied the saturated pool boiling heat transfer in a vertical narrow annulus with both ends open. They observed that there is a remarkable difference of heat transfer between the coalesced bubble regime and the isolated bubble regime. These regimes were separated by a critical gap size, which varied with fluid properties. The isolated bubble regime was present in larger crevices. Below the critical crevice dimension, the coalesced bubble regime was observed. Jensen, Cooper, and Bergles [2] performed experiments of saturated water pool boiling at atmospheric pressure in horizontal annuli utilizing an electrically heated inner surface. Crevice heat transfer coefficients were as much as 230 % greater than those measured for conventional pool boiling. The increase in the heat transfer was explained by the thin film evaporation. The critical heat flux was found to be directly proportional to the gap size and inversely proportional to the length of annulus. However, Jensen et al. did not report detailed visual observations in the narrow crevice. Yao and Chang [3] presented a series of systematic

investigations of pool boiling heat transfer in vertical narrow annuli with closed bottoms. They found that the Bond number is important in characterizing the boiling behavior in confined spaces.

The primary objective of this research is to perform a systematic investigation of pool boiling heat transfer in narrow horizontal annuli with various working fluids. Visual observation will also be performed to assist the explanation and the correlation of the heat transfer results.

EXPERIMENTAL APPARATUS AND PROCEDURE

Experiments will be performed in horizontal pools of various fluids, such as Freon-113, Acetone, and distilled water. The electrically heated tube is placed inside a hollow quartz cylinder with a small concentric gap maintained in between. The entire structure is positioned horizontally with the annulus left opened to the fluid pool at both ends. The overall test assembly is shown in Figure 1 and a schematic of the test section appears in Figure 2.

The liquid pool would be established using a Pyrex tube of 101.6 mm inside diameter and 457.5 mm length. The generated vapor in the boiling experiments will be released to a separate condenser. The liquid level will be maintained by an equalizer which is connected to the pool, and the saturation temperature of the pool will be maintained by an immersion heater.

Before each experiment the pool liquid will be degassed by boiling for one hour at a low heat flux. The movable thermocouples with 0.81 mm

diameter are pressed against the inner-wall of the central tube by springs. The thermocouples can be traversed axially and rotated at the interior of the heated tube to measure the boiling heat transfer.

The experiment will be performed for various gap sizes and axial lengths. The boiling behavior will be presented and compared with those observed by Ishibashi & Nishikawa [1], Jensen et al. [2] and Yao & Chang [3]. The effects of fluid properties and gap sizes on boiling phenomenon will be studied and discussed. A movie series will be edited.

CURRENT STATUS

The test facility and the test section have been fabricated and assembled. Try runs will be performed in the near future.

REFERENCES

1. E. Ishibashi and K. Nishikawa, "Saturated Boiling Heat Transfer in Narrow Spaces," *Int. J. Heat Mass Transfer*, Vol. 12, pp. 663, 1969.
2. Jensen, M. K., Cooper, P. E. and Bergles, A. E., "Boiling Heat Transfer and Dryout in Restricted Annular Geometries," 16th National Heat Transfer Conference, *AIChE*, Paper No. AIChE-14, pp. 205, 1976.
3. S. C. Yao and Y. Chang, "Pool Boiling Heat Transfer in Confined Spaces," Submitted to *Int. J. Heat Mass Transfer*, March 1982.

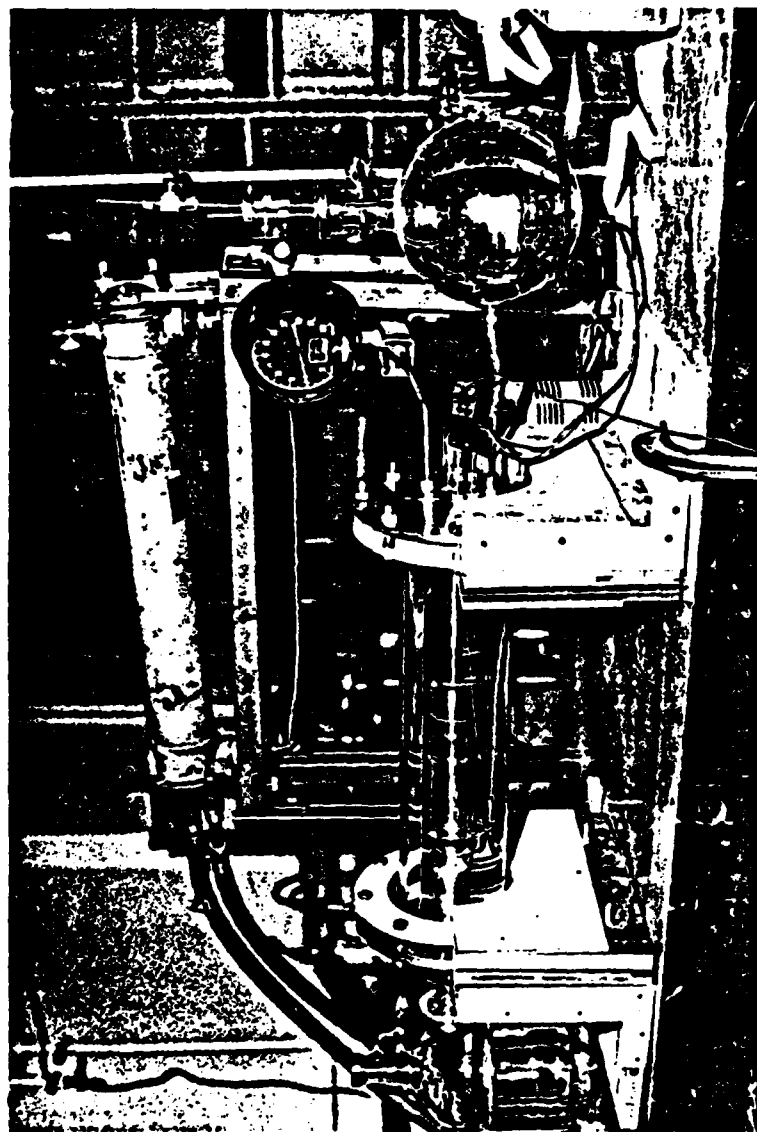


Fig. 1. The Overall Test Assembly

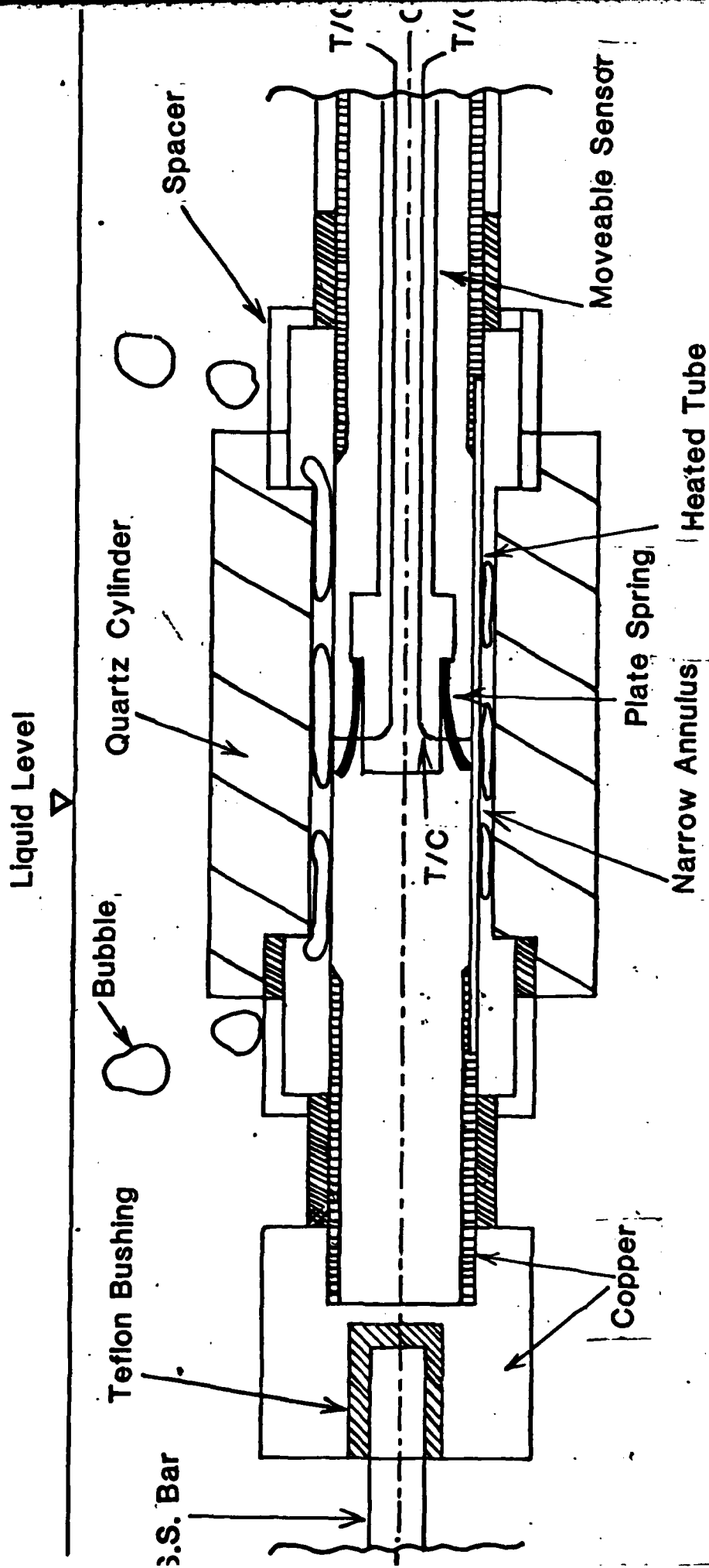


Fig. 2 Schematic of the Test Section

CHAPTER 4
CROSS FLOW BOILING IN TUBE BUNDLES

CROSS FLOW BOILING IN TUBE BUNDLES

INTRODUCTION

In many of the power systems of Naval vehicles the steam generators contain tube bundles which are oriented horizontally. Boiling occurs in the shell side as shown in Figure 1. The tubes can be arranged in triangular array or in square array at a particular pitch-to-diameter ratio which determines the tube to tube spacing. Steam and water flows in the steam generator crossing the tube bundle by the gravity induced natural convection. However, at any position in the bundle the boiling heat transfer on the tube is mainly dependent of the local flow velocity and the local quality. The study of heat transfer in a particular region of a large bundle can, therefore, be performed in a smaller bundle at a forced convective boiling condition with the same velocity and quality condition.

The heat transfer knowledge of tube bundles has been greatly advanced in the last decade due to the intensive research on nuclear reactor thermal hydraulics. However, almost all of the published information is for the condition of axial flow along the tube bundles because all nuclear reactor bundles are cooled by the fluid at axial flow. The knowledge of heat transfer in tube bundles at cross flow conditions is very limited. In fact, the available information is mainly originated from the reboiler design in chemical processes.

Interesting but not very much relevant information is available from the

abundant literature on the heat transfer of a single tube at cross flow. Fundamental understanding and parametric effects are revealed, however, the result is so far away from the practical application of the heat transfer in tube bundles. The major difference between the single tube heat transfer and the heat transfer on a tube in a heated bundle is the different flow field and thermal field near the tube.

For a better understanding of the cross flow boiling in tube bundles, systematic study is necessary. The study should be able to bridge the knowledge of single tube heat transfer to the bundle heat transfer, and to compare the heat transfer of triangular array bundle to square array bundle. The effect of thermal environment adjacent to a tube in the bundle should also be studied by comparing the results of one tube heated vs. all tubes heated, single phase vs. two phase flow at different quality, as well as the study of the effect of velocity to boiling heat transfer.

The systematic research on the subject is in progress at the Thermal Science Laboratory in Carnegie-Mellon University. The Freon loop which has been used previously for the study of boiling in confined spaces needs to be modified to give higher flow rate and high inlet two phase quality to the test section. The recording of abundant experimental data from the test bundle also requires more sophisticated data acquisition system.

For this reason, the major effect in the last year is to rebuild the test loop and data acquisition system, to design the test section and to pre-test the design concept.

Till now, the loop has already been reconstructed. The new data

acquisition system was established. The design of the test section has been finished and pre-testing of the tubes gives satisfactory results as expected. The following section describes the detail of the experimental facilities.

FREON LOOP

The objective of the loop modification is to achieve a wide range of operation condition. The schematic of the modified loop is presented in Figure 2 and with its specifications described in Table 1.

The piping and fittings are mainly made of type 304 stainless steel. Freon-113 is circulated by a Crane stainless leakage-proof dynapump, model JB-3K, which provides a discharge pressure of 80 psig at 30 GPM. After the pump, the flow is divided to the by-pass line and the test section line. In the test section line, fluid flows through the turbine flow meter, the preheaters, the main regulating valve, and the test section. After the test section, the fluid merges with the flow from the by-pass line. The mixed flow then goes through the condenser, degassing tank, and then flows back to the pump. Two Grainger filters are installed parallelly at by-pass suction line of the pump.

The flow rate through the test section is adjusted by the valve at by-pass line and the valve at the exit of the test section. Pump operation pressure is controlled by the valve at the outlet of the pump. The regulating valve at the inlet of test section is used to generate bubble required two phase quality to the test section.

The preheaters consist of four Chromalox heaters. The first and second preheaters are Model ARMTO-3605T2, each with a rated output of 6 KW at 240V. The third and fourth are Model MTO-390A of 9 KW each. Each preheater is able to provide a continuously variable power using variac. The preheater arranged in a way to prevent the burn out by trapping bubbles in the preheater casings. The second preheater is laying on the top of first preheater. The fourth preheater is installed above the third one with a 10 degree inclination.

The condenser is of a shell and tube type with Freon-113 flowing in the shell side and cooling water in the tube side. The valve on the water line is able to adjust the water flow rate and subsequently to control the temperature of Freon-113 at the pump inlet. From the condenser, Freon-113 enters the degassing tank.

A photograph of the loop assembly is shown in Figure 3. The operation condition for present study is shown in Table 2.

POWER SUPPLY

The D.C. electrical power for the heating of the test section is provided from a small welder and a large Westinghouse power supply in the Thermal Science Laboratory. The small welder supplies the finely control led power up to 40 V, 300 Amp., while the large Westinghouse power supply gives up to 100 V and 1500 Amp.. A current shunt is installed in series with the test section such that the high current input to the test section can be accurately measured.

TEST SECTION

Six different test sections will be fabricated for geometries A, B, C, D, E, and F as shown in Figure 4. These geometries are described in Table 3. The tubes will be reused and the casing is a same one.

The schematics of the overall test section is shown in Figure 5. The typical cross-section of the test section is shown in Figure 6. The changeable back plate, made of type 304 stainless steel, is fitted with tubes of 19.05 mm (3/4 inches) diameter, and 0.508 mm (0.020 inches) wall thickness. The electrically heated tubes are silver-soldered onto copper ends. The details of the tube assemblies is shown in Figure 7.

The local heat transfer on the heated tube is measured by J-type ungrounded stainless sheathed thermocouples with 0.794 mm (1/32 inches) diameter. Thermocouples and pressure taps are installed at different locations in the test section.

The casing of test section is a 127 mm (5 inches) by 76.2 mm (3 inches) rectangular Aluminum duct with 660.4 mm (26 inches) length. Glass windows are located at several positions for lighting and observation. As described in Table 3, the test bundle consists of an upstream unheated section, a heated section, and an exit unheated section. The tubes in inlet unheated section are made of solid Aluminum tubes, while the tubes in exit unheated section are made of type 304 stainless steel tubes.

Both the bottom plenum and the top plenum are made of stainless steel pipes of 101.6 mm (4 inches) diameter, 101.6 mm (4 inches) length. The bottom plenum contains two perforated plates to uniformize the inlet vapor and liquid distribution to the test bundle. The top plenum contains flow straighteners to prevent the uneven flow distribution near the top of the bundle.

INSTRUMENTATION

All the measured temperatures in the test section are recorded by the Accurex Autodata logger model 10/5. The data processing is programmed with a connected Zenith-19 cathode ray terminal. Figure 8 shows a photograph of the instrumentation rack. The system temperature in the loop can be read from two digital temperature indicators and two digital millivoltmeters.

The flow rate through the test section is measured with a turbine flow meter (Model 80-0750, manufactured by Engineering Measurement Company Inc.). The output from the turbine flow meter is recorded by a Leeds & Northrop Model Speedomax H chart recorder.

The system pressure is measured from two bourdon pressure gages. The differential pressure is measured by differential pressure transducer.

Item no.	Description
1	Regulating valve
2	Test section
3	Ball valve
4	Condenser
5	Global control valve
6	Degassing Tank
7	Filter
8	Pump
9	Turbine flow meter
10	Preheater 1
11	Preheater 2
12	Preheater 3
13	Preheater 4
14	Freon-113 Supply tank
15	Freon-113 Accumulator

Table 1: Components of the Freon-113 loop

- (1) Test Section: 60 x 85.725 x 660.4 mm
- (2) Channel flow area: 51.44 cm²
- (3) Heating condition: (max. 24 tubes heated)
heat flux: 0 - 663 kw/m²
- (4) Flow condition:
 - Superficial velocity (liquid equivalent)
0 - 0.36 m/sec
 - Volumd flow rate: 0 - 30 GPL GPM Volume
 - Mass flux: 0 - 520 kg/m²-sec
- (5) System pressure: Max. 40 psig

Table 2: Operation condition

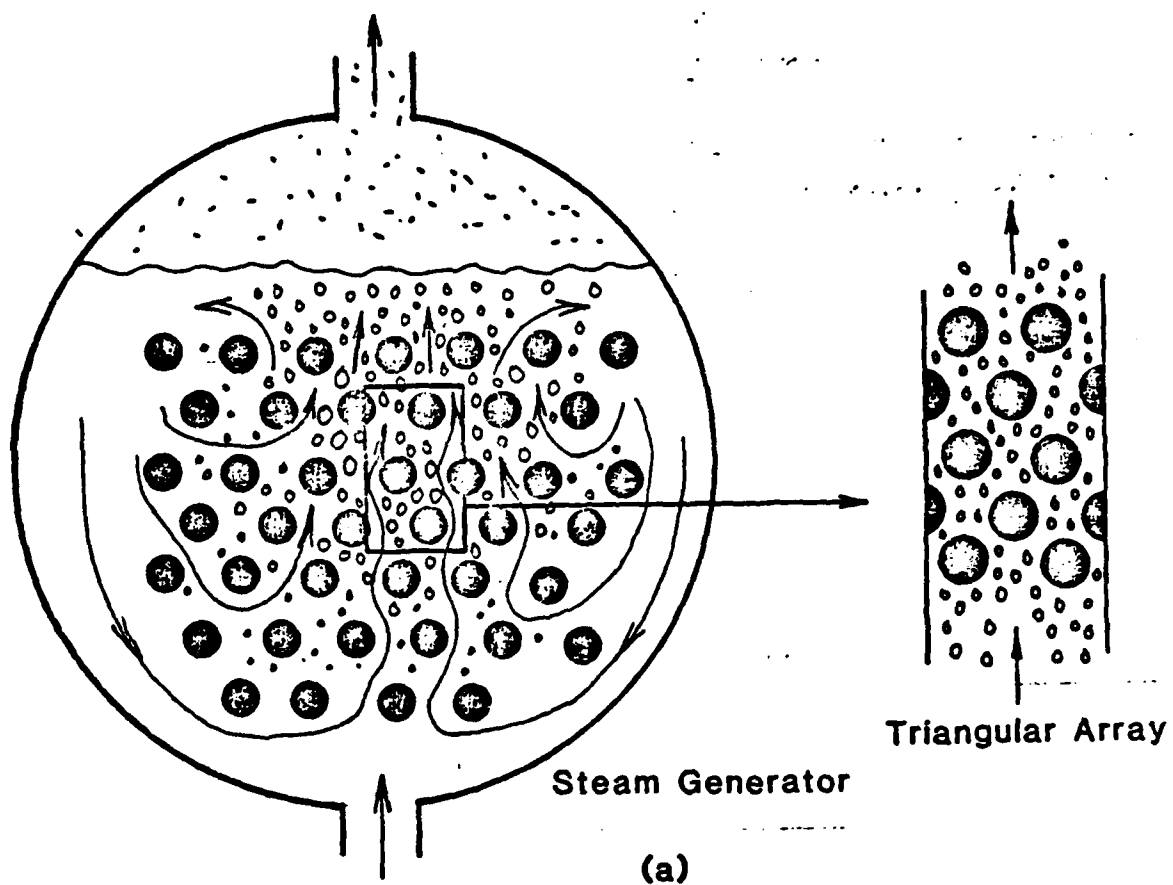
Test-Section Configuration

		A	B	C	D	E	F
	Exit Zone	0	2	3	3	3	3
No. of Rows	Heated Zone	4	6	8	8	8	8
	Transition Zone	2	4	6	6	6	6
No. of Columns		1	2	3	3	2	2
Pitch to Diameter Ratio		4.5	2.25	1.5	1.5	1.5	1.5
Pitch (mm)		85.725	42.8625	28.575	28.575	28.575	28.575

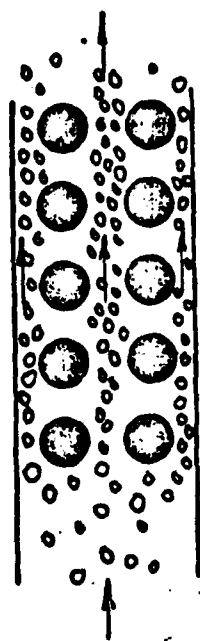
Tube diameter: 19.05 mm

Tube length: 60 mm

Table 3: Test-section Description



Triangular Array



Vapor Streaming in Square Array

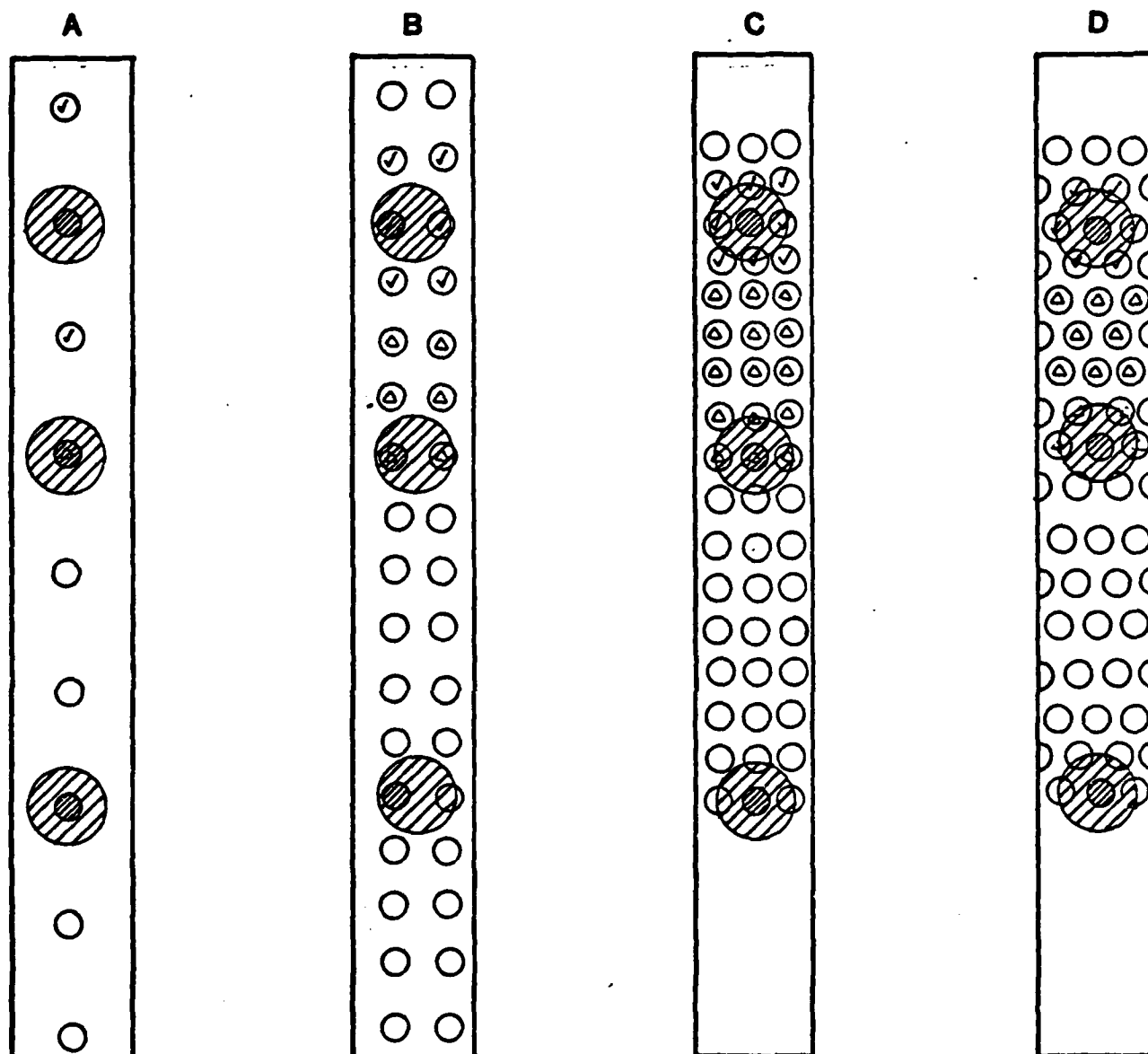
(b)

Fig. 1

Fig 2: Schematic of Freon-113 loop.



Fig 3: photo of Freon-113 loop



- DUMMY RODS
- INSTRUMENT RODS
- ✓ MAIN ADJACENT HEATED TUBE
- △ PRE-HEATED TUBES

Fig 4: Configuration of test sections

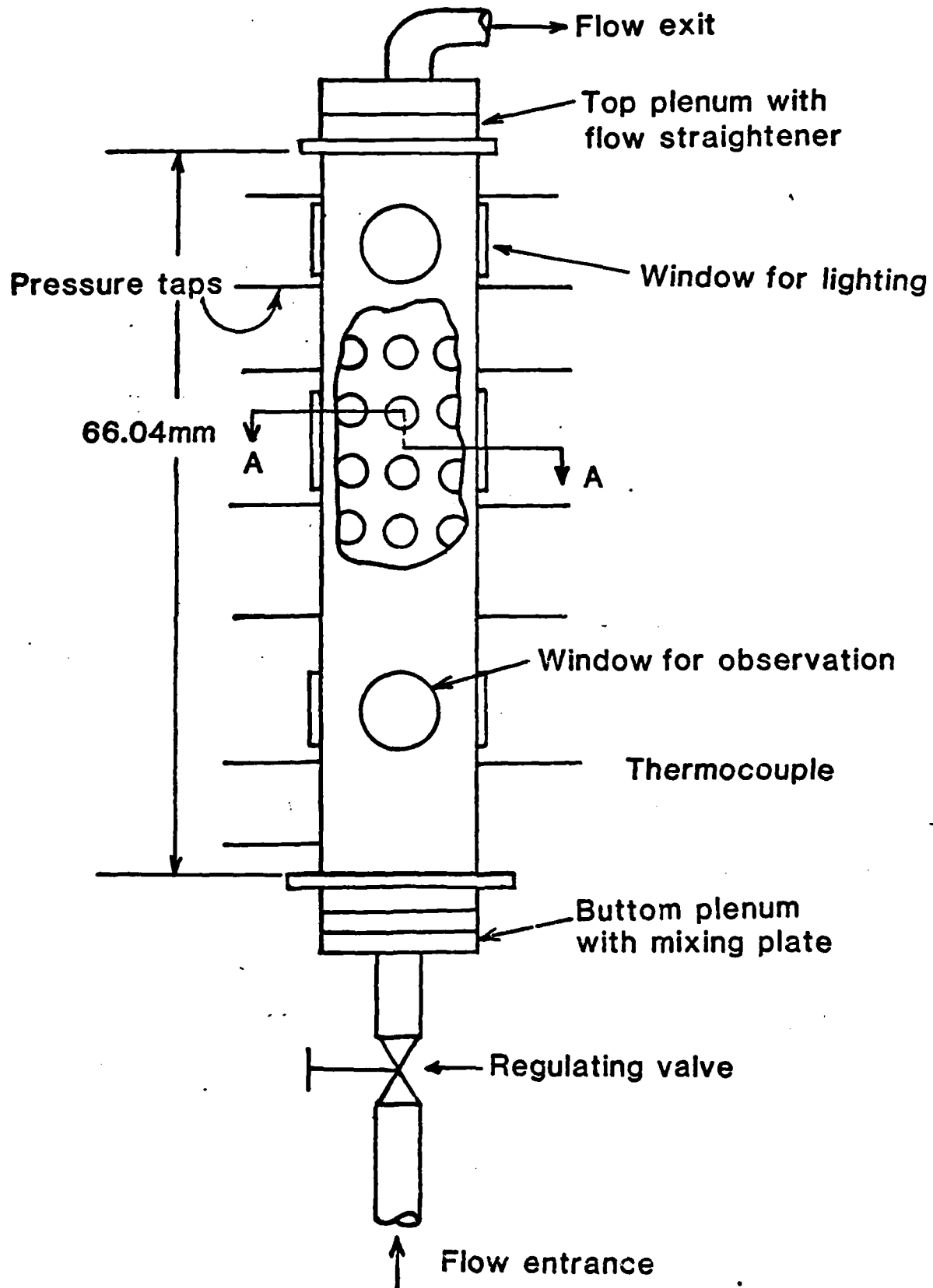


Fig 5: Test-section Schematic

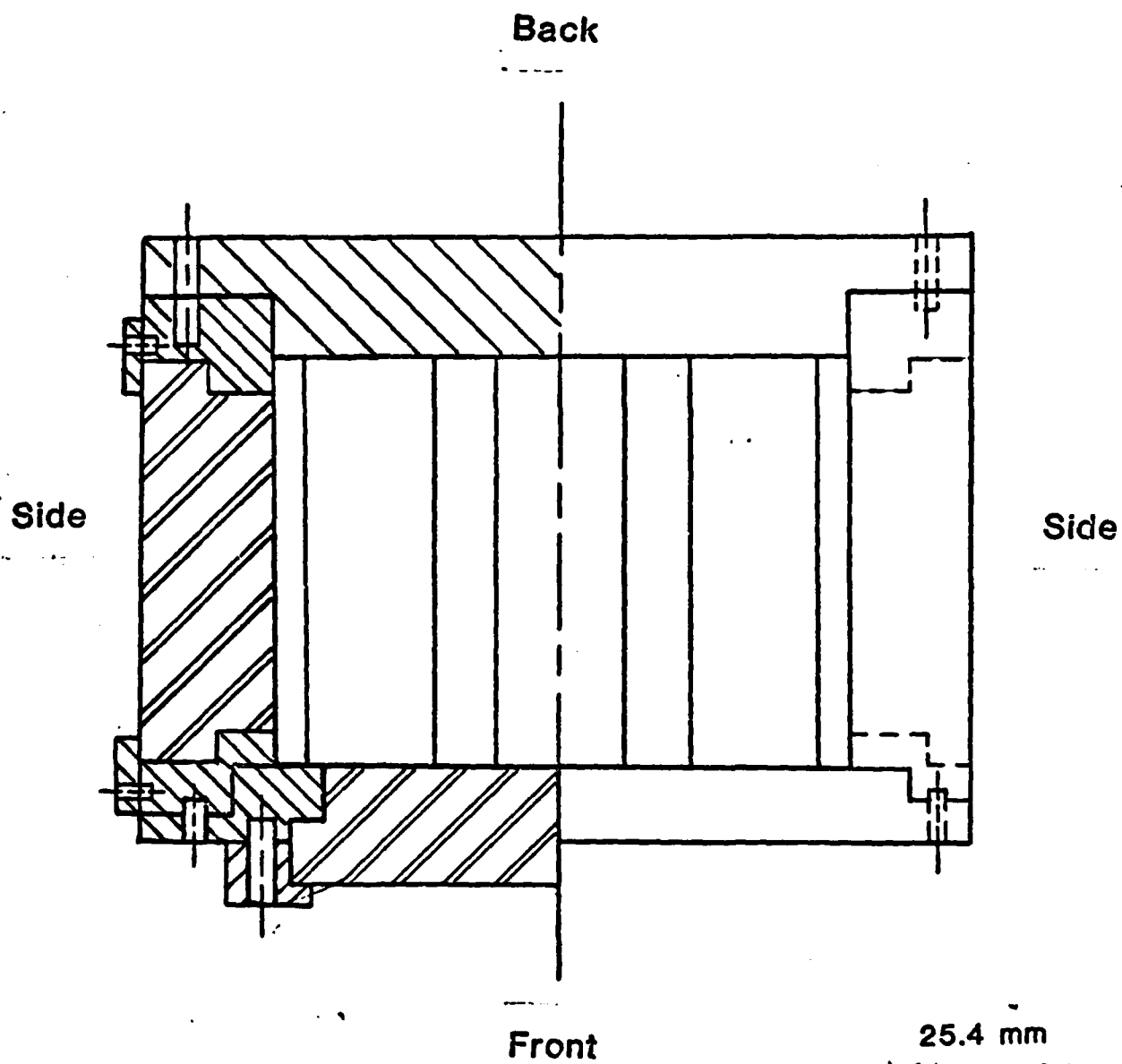


Fig6: Cross-section of Test-section
(view A-A)

$3 \times \square = P/D = 1.5$

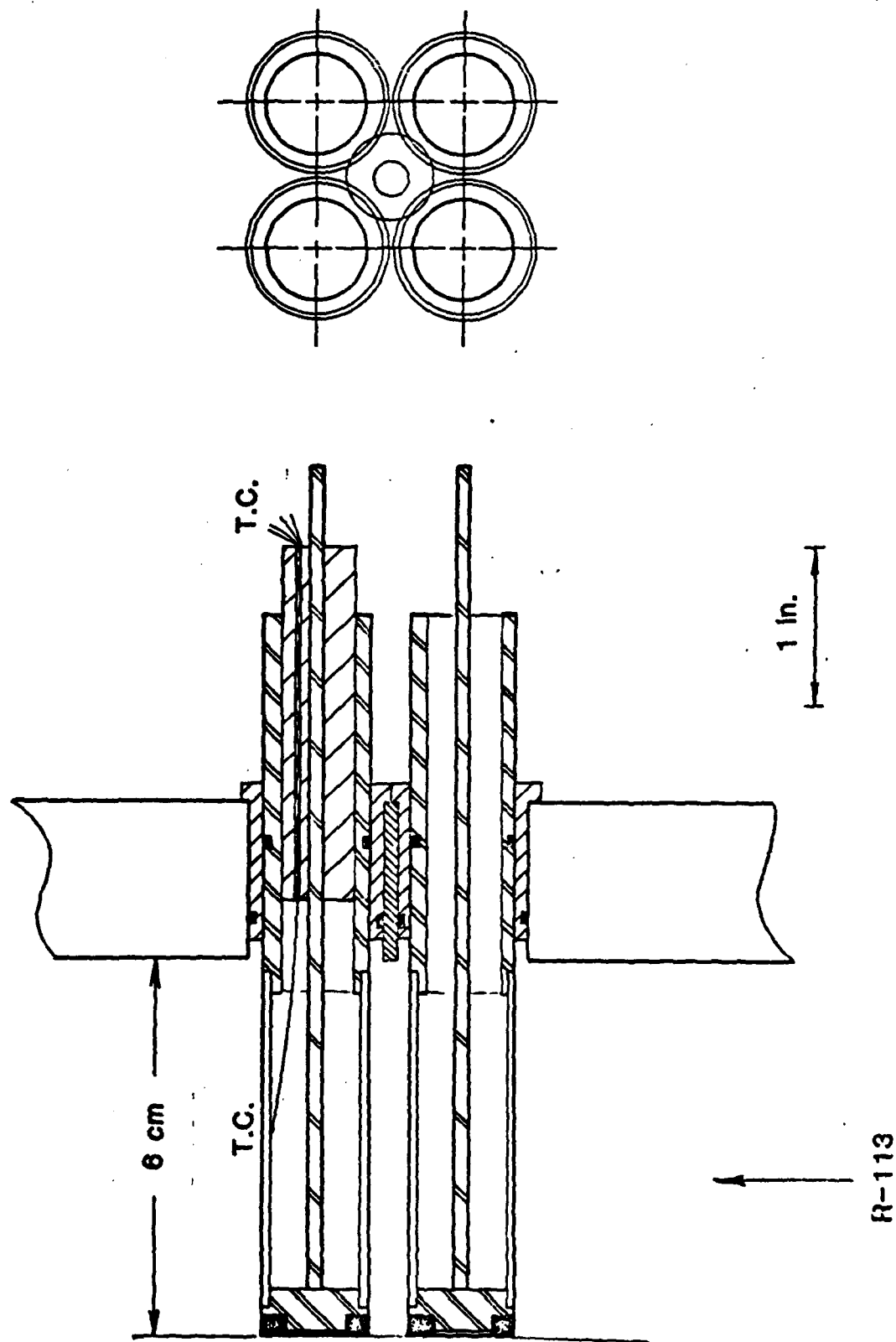


Fig 7: Assembly of heated tube

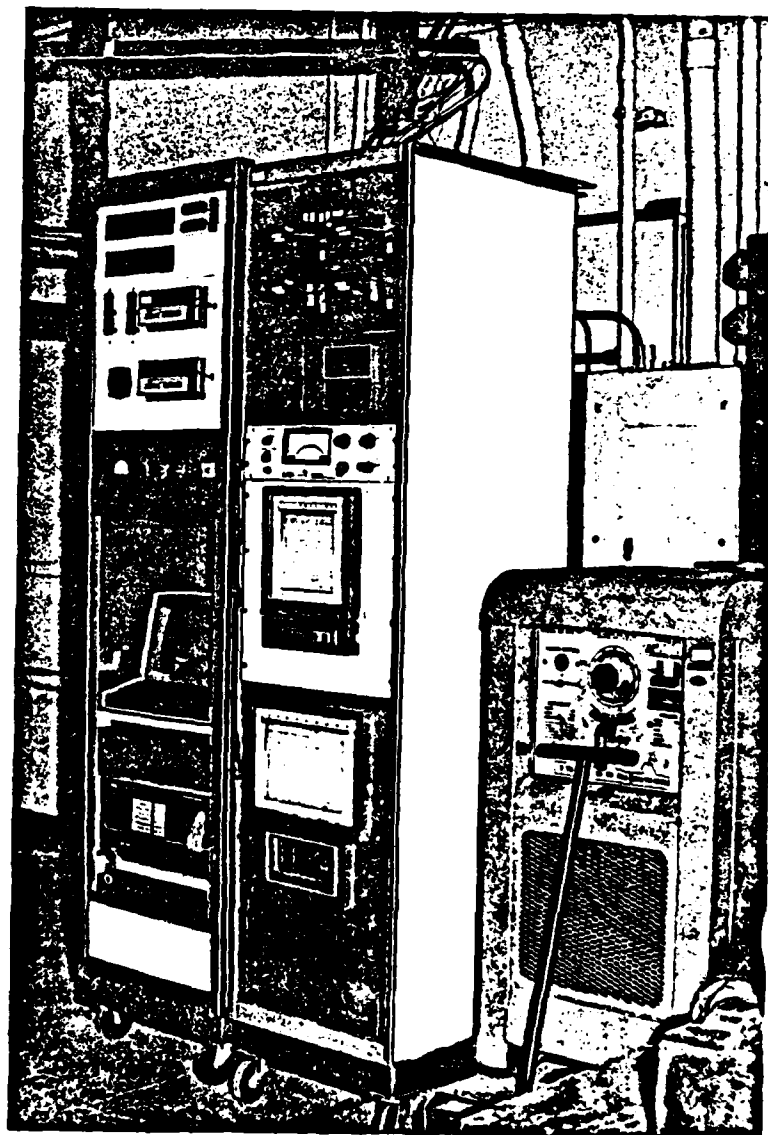


Fig 8: Photo of racks

AD-A121 510

CROSS FLOW BOILING IN TUBE BUNDLES(U) CARNEGIE-MELLON
UNIV PITTSBURGH PA DEPT OF MECHANICAL ENGINEERING
S YAO OCT 82 N00014-79-C-0623

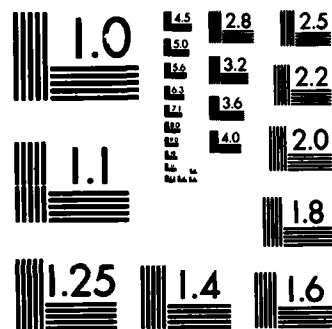
2/2

UNCLASSIFIED

F/G 20/13

NL

						END
						TO MED
						A
						DTM



MICROCOPY RESOLUTION TEST CHART
NATIONAL BUREAU OF STANDARDS-1963-A

DISTRIBUTION LISTHEAT TRANSFER

One copy except
as noted

Mr. M. Keith Ellingsworth
Power Program
Office of Naval Research
800 N. Quincy Street
Arlington, VA 22217

5

Defense Documentation Center
Building 5, Cameron Station
Alexandria, VA 22314

12

Technical Information Division
Naval Research Laboratory
4555 Overlook Avenue SW
Washington, DC 20375

6

Professor Paul Marto
Department of Mechanical Engineering
US Naval Post Graduate School
Monterey, CA 93940

Professor Bruce Rankin
Naval Systems Engineering
US Naval Academy
Annapolis, MD 21402

Office of Naval Research Eastern/
Central Regional Office
Bldg 114, Section D
666 Summer Street
Boston, Massachusetts 02210

Office of Naval Research Branch Office
536 South Clark Street
Chicago, Ill. 60605

Office of Naval Research
Western Regional Office
1030 East Green Street
Pasadena, CA 91106

Mr. Charles Miller, Code 05R13
Crystal Plaza #6
Naval Sea Systems Command
Washington, DC 20362

Enclosure (2)

37
Steam Generators Branch, Code 5222
National Center #4
Naval Sea Systems Command
Washington, DC 20362

Heat Exchanger Branch, Code 5223
National Center #3
Naval Sea Systems Command
Washington, DC 20362

Mr. Ed Ruggiero, NAVSEA 08
National Center #2
Washington, DC 20362

Dr. Earl Quandt Jr., Code 272
David Taylor Ship R&D Center
Annapolis, MD 21402

Mr. Wayne Adamson, Code 2722
David Taylor Ship R&D Center
Annapolis, MD 21402

Dr. Win Aung
Heat Transfer Program
National Science Foundation
Washington, DC 20550

Mr. Michael Perlsweig
Department of Energy
Mail Station E-178
Washington, DC 20545

Dr. W.H. Theilbahr
Chief, Energy Conservation Branch
Dept. of Energy, Idaho Operations Office
550 Second Street
Idaho Falls, Idaho 83401

Professor Ephriam M. Sparrow
Department of Mechanical Engineering
University of Minnesota
Minneapolis, Minnesota 55455

Professor J.A.C. Humphrey
Department of Mechanical Engineering
University of California, Berkeley
Berkeley, California 94720

Professor Brian Launder
Thermodynamics and Fluid Mechanics Division
University of Manchester
Institute of Science & Technology
P088 Sackville Street
Manchester M601QD England

Professor Shi-Chune Yao
Department of Mechanical Engineering
Carnegie-Mellon University
Pittsburgh, PA 15213

Professor Charles B. Watkins
Chairman, Mechanical Engineering Department
Howard University
Washington, DC 20059

Professor Adrian Bejan
Department of Mechanical Engineering
University of Colorado
Boulder, Colorado 80309

Professor Donald M. McEligot
Department of Aerospace and Mechanical Engineering
Engineering Experiment Station
University of Arizona 85721

Professor Paul A. Libby
Department of Applied Mechanics and Engineering Sciences
University of California San Diego
Post Office Box 109
La Jolla, CA 92037

Professor C. Forbes Dewey Jr.
Fluid Mechanics Laboratory
Massachusetts Institute of Technology
Cambridge, Massachusetts 02139

Professor William G. Characklis
Dept. of Civil Engineering and Engineering Mechanics
Montana State University
Bozeman, Montana 59717

Professor Ralph Webb
Department of Mechanical Engineering
Pennsylvania State University
208 Mechanical Engineering Bldg.
University Park, PA 16802

Professor Warren Rohsenow
Mechanical Engineering Department
Massachusetts Institute of Technology
77 Massachusetts Avenue
Cambridge, Massachusetts 02139

Professor A. Louis London
Mechanical Engineering Department
Bldg. 500, Room 501B
Stanford University
Stanford, CA 94305

Professor James G. Knudsen
Associate Dean, School of Engineering
Oregon State University
219 Covell Hall
Corvallis, Oregon 97331

Professor Arthur E. Bergles
Mechanical Engineering Department
Iowa State University
Ames, Iowa 50011

Professor Kenneth J. Bell
School of Chemical Engineering
Oklahoma State University
Stillwater, Oklahoma 74074

Dr. James Lorenz
Component Technology Division
Argonne National Laboratory
9700 South Cass Avenue
Argonne, Illinois 60439

Dr. David M. Eissenberg
Oak Ridge National Laboratory
P.O. Box Y, Bldg. 9204-1, MS-0
Oak Ridge, Tennessee 37830

Dr. Jerry Taborek
Technical Director
Heat Transfer Research Institute
1000 South Fremont Avenue
Alhambra, CA 91802

Dr. Simion Kuo
Chief, Energy Systems
Energy Research Laboratory
United Technology Research Center
East Hartford, Connecticut 06108

Mr. Jack Yampolsky
General Atomic Company
P.O. Box 81608
San Diego, CA 92138

Mr. Ted Carnavos
Noranda Metal Industries, Inc.
Prospect Drive
Newtown, Connecticut 06470

Dr. Ramesh K. Shah
Harrison Radiator Division
General Motors Corporation
Lockport, New York 14094

Dr. Ravi K. Sakhuja
Manager, Advanced Programs
Thermo Electron Corporation
101 First Avenue
Waltham, Massachusetts 02154

Mr. Robert W. Perkins
Turbotec Products, Inc.
533 Downey Drive
New Britain, Connecticut 06051

Dr. Keith E. Starner
York Division, Borg-Warner Corp.
P.O. Box 1592
York, PA 17405

Mr. Peter Wishart
C-E Power Systems
Combustion Engineering, Inc.
Windsor, Connecticut 06095

Mr. Henry W. Braum
Manager, Condenser Engineering Department
Delaval
Front Street
Florence, New Jersey 08518

Dr. Thomas Rabas
Steam Turbine-Generator Technical Operations Division
Westinghouse Electric Corporation
Lester Branch
P.O. Box 9175 N2
Philadelphia, PA 19113

Professor Daryl Metzger
Chairman, Mechanical and Energy
Systems Engineering
Arizona State University
Tempe, Arizona 85281